APPLICATION OF REMOTE SENSING AND GIS FOR GEOLOGICAL INVESTIGATION AND GROUNDWATER POTENTIAL ZONE IDENTIFICATION, SOUTHEASTERN ETHIOPIAN PLATEAU, BALE MOUNTAINS AND THE SURROUNDING AREAS

By

Tewodros Rango Godebo

Faculty of Natural Science

Department of Earth Sciences

APPROVAL BY BOARD OF EXAMINERS

Dr. Dereje Ayalew _____

Chairman, Department

Graduate Committee

Dr. Tesfaye Korme _____

Advisor

Dr. Dereje Ayalew _____

Co-Advisor

Dr. Daniel Mege _____

Co-Advisor

Dr. Syed Ahmad Ali _____

Examiner

Dr. K.S.R Murty _____

Examiner

ACKNOWLEDGEMENT

I would like to express my sincere gratitude to Ministry of Finance and Economic Development for providing me the financial support to pursue this higher-level education in Addis Ababa University, Department of Earth Sciences under Remote Sensing and GIS stream.

I am greatly indebted to Dr. Tesfaye Korme and Dr Daniel Mege for sharing their scientific knowledge especially during my fieldwork. I want to thank Dr. Tarun K. Raghuvanshi for his support in solving problems I encountered during preparation of some of data. Again, I extend my thanks to Dr. Daniel Mege, Lucy Tallents (PhD student) and Bale Mountains National Park (BMNP) for providing me supportive ideas and the photographs I used in my thesis. I thank those employees in the park for assisting us during fieldwork. I want to thank Mr. Adisa from Geological Survey of Ethiopia for sharing his knowledge for laboratory analysis of thin sections.

I always feel grateful, proud and strong for having very decent friends Dereje Getahun and Zeleke Kebebew that I shared much knowledge during my thesis work and for discussing different aspects of life. My thanks also go to Dr. Behailu Atlaw and Mr. Zekarias Mama for their constructive advice and support in my life and education. I would also thank Mehaza Bekele for her supportive activities. I thank all my friends in RS\GIS department for good time we passed together in the last two years. I greatly thank my classmate Addisu Dereje for his assistance at the end of my thesis work in preparing the thesis in proper format. I would thank also my sister Mehalet and Fitsum M. for doing some of the write up. I thank all I missed to mention their name but contribute the thesis to be successful.

Above all, I thank God, his ever-lasing words that makes thing to be possible.

LIST OF FIGURES

LIST OF TABLES

ABSTRACT

The application of remote sensing and GIS has found to be a quick and inexpensive technique in order to obtain the desired output efficiently. For the present study an attempt was made to map dykes, lithology and other thematic maps such as of drainage density, slope, elevation, lineament, rainfall, landcover and burrowing of rodents and then to integrate them in a GIS environment to get information about the occurrence of groundwater and used to select promising areas for further groundwater exploration.

The present study was conducted on southeastern part of Ethiopia plateau, the Bale Mountains and the surrounding areas. Satellite image of Landsat ETM+ of all bands except the thermal bands were utilized for lithologic and geologic structures mapping. Topographic map at the scale of 1:50,000 were used to generate elevation contour at the interval of 20m. Slope map were derived from TIN (Triangulated Irregular Network), which is derived from elevation contour map. Spatial distribution of drainage density was derived by using three softwares AutoCAD map 2000 engineering software, Arcview3.2 and MapInfo professional 6.0. The burrowing of Rodents were mapped from field Knowledge and using 742(RGB) that shows areas of rodent burrowing activities. Secondary data of landcover, soil were also utilized. Groundwater potentiality in the area has been assessed through the integration of the different thematic layers that contributes for the natural recharging of aquifer. The predicted groundwater potential zones were divided into 5 classes from very good up to poor.

Color composite, ratio and PCA (Principal Component analysis) were made to interpret the lithology of the area. Due to vegetation cover and similarities of reflectance of different rock units it was difficult to separate them. The field knowledge and some petrographic analysis support the identification of the lithology.

Key words: dykes, lithology, groundwater potential zone prediction, Remote Sensing and GIS

TABLE OF CONTENT

visualizing, querying, combining, or generally analyzing data, or by making predictions with the data (Bonham-Carter, 1994). A critical factor governing the incorporation of remotely sensed data into a GIS is the digital nature of the data (Legg, 1994).

There are two general approaches for using remote sensing in mineral explorations (Sabins, 1999). One approach is to map geology and structures at regional and local scale; the other is to recognize hydrothermal alterations that can be associated to mineral deposits. Because geology, structure, and hydrothermal alterations can be used as indications of the presence of mineral deposits, the combination of both approaches, which can be done in a GIS, is the most efficient. In addition, topographic data in the form of Digital Elevation Models (DEM) can be combined with remotely sensed imagery to map geological features indicative of mineralization of the type sought (Rokos et al., 2000). Likewise, the concept of integrated remote sensing and GIS techniques has proved to be an efficient tool in groundwater studies (Krishnamrthy et al 1996, Saraf and Chaudhary 1998, Khan and Mohrana, 2002)

The study area is covered by hard rock terrain; the occurrence of groundwater in this type area can be effectively mapped using the integration of thematic maps generated from remotely sensed data on a model developed based on GIS techniques. The thematic maps include geological structures (dykes, faults and lineaments), drainage density, slope, elevation, soil type, landcover, annual rainfall and biological factors (burrowing of rodents). The integration of the thematic layers will be performed using the techniques of overlay analysis.

The study of dyke composition, geometry and associated planar regional fracture in the Ethiopian plateaus can greatly help in locating hydrothermal vein minerals and groundwater recharge and discharge zones. The main recharge zones of groundwater in the near by drought prone lowlands is the dykes and fracture system on the plateau. Fracture analysis is one of the major techniques used in the exploration of groundwater in crystalline rocks and hydrothermal mineralization. The application of remote sensing and geographic information system is one of the most effective techniques in mapping fractures and dykes, hydrothermal alteration zones, drainage network, soil type, slope steepness, topographic height, landuse/landcover and lithology and allow integrating them in a spatial environment. Therefore, the study of groundwater and mineral potential of the area is crucial for the economic development of both the plateau and adjacent lowland areas. It could help the national poverty reduction strategy in locating precisely the places for drilling to

obtain sustainable groundwater supply for irrigation, consumption, crops and livestock production, and in locating hydrothermal alteration areas on the plateau.

1.2. The study area

Southeastern Ethiopian Plateau, namely Arsi-Bale Mountains is located south east of Addis Ababa. It is bounded by 39º33'41.59"-39º58'46.42" longitudes (561850E-607744E) and 6º40'24.67-7º16'5".53" latitude (737740N-803375N). The access to the area is either using Addis Ababa-Nazareth-Asela-Goba road or Addis Ababa-Shashemene-Assassa–Goba road.

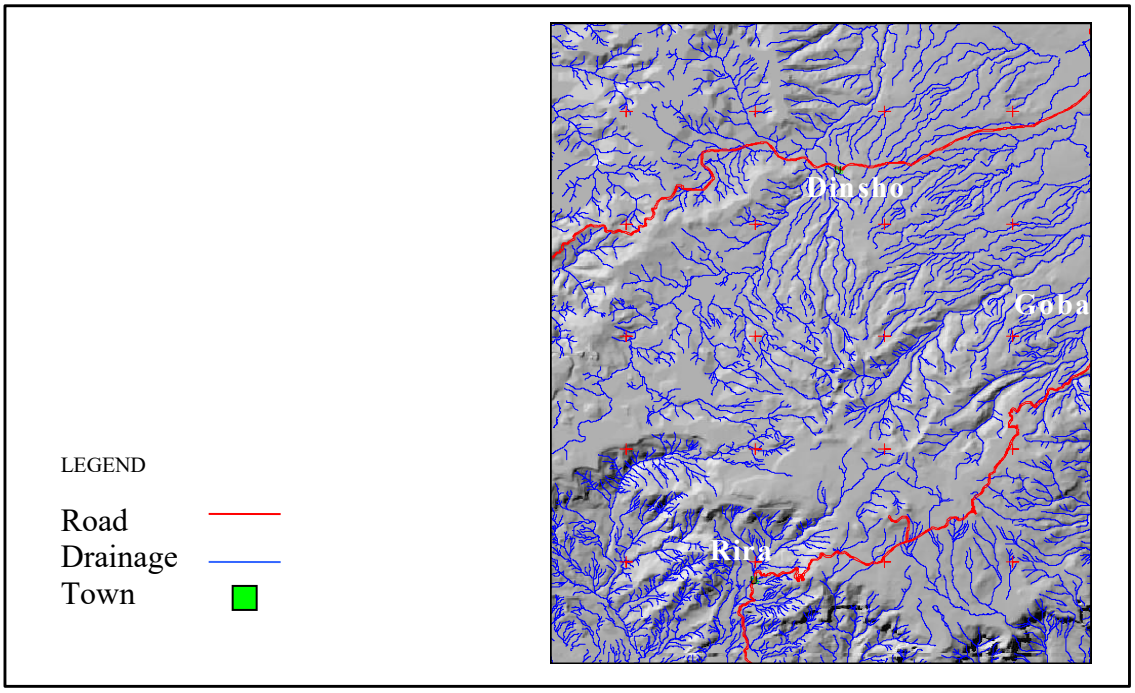

Figure 1.1. Location map of the study area, Bale Mountains and the surrounding

1.2.1. Glaciations

Former glaciations have considerably modified the volcanic landscape of the Bale Mountains. Traces of former glaciers are common in the Ericaceous and Afro-alpine Belts: ice striations, glacial cirques and tongue basins with recent swamps or lakes, and moraines (clearly observed at Sebsebe washa, left side of the road from Dodola to Dinsho) that characterizes unsorting, loosely consolidated sediments of varying size and shape and angular and sub angular fragments. Deep valleys of smoothed U-shaped cross-section are indicators of the presence of former glaciations

on the mountains. Mt. Badda, 100km North of the Sanetti plateau, was a significant center of alpine glaciation in the Pleistocene (Potter, 1975). He also noted that only a few, very high mountains in eastern Africa with peaks generally over 3500m.a.s.l are known to have been glaciated. There have been at least two glacial periods in the history of the mountains but they were glaciated as little as 2000 years ago. The glaciers descended to a level of about 3000-3500m and valleys such as Togona are characteristics of glacial valleys.

1.2.2. Physiography

The Bale Mountains and the surrounding areas classified as plateau forming massifs, the Sanetti plateau and the Harenna plain and the adjacent lowlands. The altitude on the study area varies from 1760m at SW and SE corner of the Harenna forest and to the highest peak in southern Ethiopia at Tullu Dimtu, is 4377m a.s.l. EW trending the Harenna erosional escarpment lies between significant topographic variations within less than 10km distance (Figure 1.2). The edges of the flat topped Sanetti plateau are highly dissected. The slope from the foot of the escarpment southwards is relatively gentle.

The Bale Mountains, the Sanetti plateau, is characterized by extensively flat areas formed by Cenozoic volcanic rock of alkaline basaltic and trachytic lava flows that originated from vents on the plateau. The lavas flowed west wards and northwards and stopped on the edge of the present day rivers, locally forming sub-vertical step like cliffs Highly dissected country, showing ridges and intervening valleys mostly identify the plateau edges. In general the highland area marks a very important nearly E-W oriented watershed characterized by swampy areas and many small shallow lakes. The headwater of Genale and WabeShebele rivers also emanate from this plateau. The rivers on the study area lie with in these river basins.

Figure 1.2. The Herenna escarpments

1.2.3 Climate

Significant variation in climate resulted from great variation in altitude and the bulk of the massif over the area of the Bale Mountains attracts large amounts of orographic rainfall.

1.2.3.1. Rainfall

In general, the rainfall in the area is characterized by one eight-month rainy season-from march to October, followed by a four-month dry season-from November to February. Precipitation falls on the high altitude plateau during the dry, cold season is in the form of sleet or snow. This general pattern differs only in the far south and lower altitudinal area, which has a shorter, four-month rainy season from February-June. The lower altitudes of the area receive between 600-1000mm of rainfall annually, whereas the higher altitudinal areas receive up to 1200mm. The rainfall is received from two directions during the rainy season-the equatorial westerlies and The Indian Ocean air streams. The Harenna plain and associated lowlands are characterized by double rainy and dry seasons. March to June and September to October are the main and lesser rainy seasons, whereas November to February and July to August are the main and lesser dry seasons, respectively (Figure 1.3).

Figure 1.3. Climate of Bale Mountains, Snow cover, Sanetti plateau.

1.2.3.2. Temperature

Temperature falls with increasing altitude. At the higher altitudes, the lowest temperatures occur at night in the clear skies of the dry season and the highest temperatures during the day during the same season. The daily temperatures during the dry season show a vast fluctuation. The lowest temperature that has been recorded in the mountains is -15^{O}C at night, with the highest recorded temperature the next day of +26^{O}C and thus a range of 40^{O}C within a 24-hour period!

In contrast, the rainy season is warmer and the temperature shows much less daily fluctuation. It rarely freezes during the rainy season but the temperature rarely climbs over 20^{O}C.

1.2.3.3. Hydrology

The Bale Mountains act as water catchments for the region. Water is the fundamental resource for all life. People, livestock and the environment in the southeast of Ethiopia and further into Somalia are dependent on the water that originates from the Bale massif. The Bale massif plays a crucial role in climate control in the region by attracting large amounts of orographic rainfall (rainfall that occurs because of the mountains nature of the area). This has obvious implication for rain fed agriculture. Over forty streams arise within the BMNP (Bale Mountains National

Park). These join to form four major rivers-the Webe Shebelle, the Web (leading to the Genale and Juba Rivers), the Welmel and Dumal Rivers. In addition, the water for the numerous springs emerging in the lowlands originates from the Bale Mountains. These rivers and springs are the only sources of perennial water for the arid lowlands of the east and southeast of Ethiopia, including the Ogaden and Somalia areas, and neighbouring Somalia.

1.2.4. Flora and Fauna

The Bale Mountains are characterized by unique and diverse natural resources. It also contains species that are endemic to Ethiopia and the mountain itself. These include the largest Afroalpine habitat on the continent. Of the area's recorded birds, 6.1% are Ethiopian endemics. There are several rare endemic species of amphibian. The area contains the largest population of the endemic mountain nyala about 1500 individuals in the Bale Mountains are estimated to be approximately half the global population. The area contains the entire global population of the giant molerat. Of the area's recorded mammals, 26% are Ethiopian endemics. The Bale Mountain is the most important area for birds in the on the country, of the areas recorded birds, 6.1% are Ethiopian endemics. The Afroalpine plateau and the Harenna forest (the second largest stand of moist and tropical forest remaining in Ethiopia) form watershed of the area. The Bale Mountains contains over half the global population of the Ethiopian Wolves. This is the rarest (Critically Endangered) canid in the world and is found only in suitable Afroalpine habitats in Ethiopia. (Figure 1.4.).

A B

Figure 1.4. Endemic animals of the Bale Mountains, the Ethiopian wolf (A) and Mountain Nyala (B)

The area can be divided into five vegetation zones: these are primarily demarcated by altitude. Each of these zones has their own characteristics flora and fauna. There is a small area of grassland in the Gaysay valley in the very north of the park. The northern slopes of the area are covered with woodland. Above this zone, there is a belt of Erica or heather. Again, above this zone lies the area of the central peaks and the plateau consisting of Afroalpine Moorland. Finally, the southern part of the area-the Herenna Forest-is dense, closed canopy forest. (Stuart Williams, 2002).

1.3. Previous work in the study area

The Bale Mountains and the surrounding area lie within Arsi-Bale Mountains of the eastern Ethiopia plateau. Unlike the western Ethiopian plateau, geological, dyke and hydrogiological investigations have been carried out to a lesser extent in the eastern Ethiopia plateau. Regional geological mapping has been published at 1:250000 scale (EIGS, 1998). This is one of the areas that provide important data on Ethiopian volcanics. In southeastern Ethiopian plateau, the Cenozoic volcanics of Bale area have been described, dated and correlated with volcanic rocks across Ethiopia Berhe et al., (1987). Based on seven new K-Ar dating Berhe et al., (1987) described the general stratigraphy of the Bale area into four major groups forming a succession of basalts and trachytes about 2000 m thick: the Lower Stratoid Basalts, the Reira Basalts, the Dodola and Aroresa Trachytes and the Sanetti basalts and Batu Trachytes. These can be considered as basic stratigraphic reference for the study area. According to Hambisa, (2000) the southeastern Ethiopian plateau, the Dodola area is built of two coexisting bimodal alkaline magma series. This includes the late Oligocene lower (pre-rift) basanite-phonolite lineage and the Mid Miocene-Late Pliocene Upper (rift-type) basanite/alkali basalt-trachyte/rhyolite lineage. The rocks are fairly porphyritic to aphyric; the essential minerals are olivine, clinopyroxene, and plagioclase in the mafic lavas, and feldspars, clinopyroxene, and titanomagnetite in the salic lavas with minor apatite and ilmenite in some rocks. The petrological and geochemical data imply that fractional crystallization is the major process responsible for the evolution of both lava series. Major elements chemistries display features agreeable with extraction of olivine, clinopyroxene, and plagioclase from mafic magmas followed by feldspars, titanomagnetite, and apatite from felsic ones. The strong similarities in Sr and Nd isotopic compositions of these lavas to basalts

from western Ethiopia, the Afar, main Ethiopian rift, and Salali (Kenya) evidently suggest that the existence of similar mantle beneath Ethiopia and Kenya.

1.4. The present research

1.4.1. Objectives

- To map in detail the dyke swarms from satellite images and analyze dyke samples composition. Remote sensing technique allows high-resolution structural mapping of extensive area in short time and low cost.
- To produce thematic maps of geological structures (dykes, faults and lineaments), drainage density, slope steepness, elevation, soil type, Landcover, and Biological factors (burrowing of rodents) from remotely sensed data, which are input for the GIS model.
- To develop a GIS model by integrating different thematic layers generated from remotely sensed and the existing data of the area in order to predict groundwater potential zones.
- To identify lithologic units using different image processing techniques.

1.5. Materials and methods

1.5.1. Materials

In order to achieve the above-mentioned objectives, the generation of new data and collection of secondary data have been carried out for the study area. The primary data derived are drainage density, lineament, elevation, slope, and the secondary data includes rainfall, land cover and soil map of the area. Remotely sensed satellite images of Landsat ETM+ data and topographic maps were used to synthesize the primary and rectify the secondary data. Table 2.1. below show the available secondary data for the study area.

Materials available	Contents	Sources	Scale of the original data
Geological map	Regional geologic units (covers central and southern portion of the study area)	Geological survey of Ethiopia.	1:250,000
Land cover map	Map of the different vegetation belts on the Bale Mountains and the cultivation areas.	Woody Biomass inventory and strategic planning	1:1,000,000
Soil map	FAO soil classification covering the study area	Woody Biomass inventory and strategic planning	1:1,000,000
Panchromatic aerial Photos	9 aerial photographs for the northern portion of the study area.	Ethiopian mapping Authority	1:50,000
Satellite images (Landsat ETM+)	Band 1, Band 2, Band 3, Band 4, Band 5 and Band 7 are used	Obtained from colleagues working on the area.	30 meter spatial resolution
Topographic maps	Elevation contour lines	Ethiopian mapping Authority	1:50,000
Meteorological data	Rainfall measurements at different stations	National Meteorological Service Agency	Unevenly distributed rainfall stations.

Table 2.1. Summary of the data used for the study

1.5.1.1. Remote sensing data

The remote sensed data used for this study are Landsat ETM+ (Enhanced Thematic Mapper Plus) and aerial photographs. The Landsat ETM+ has different spectral and spatial resolutions. The spectral bands ranges from the panchromatic data having 15 m spatial resolution, six bands in the visible, near-IR, and mid-IR spectrum at a resolution of 30 m and one thermal band at 60m resolution. For the purpose of this study only visible, near-IR, and mid-IR band and a few aerial photographs were considered. The Landsat 7 ETM+ images of the study area lies on two scenes having path/row as 167/55 and 168/55, each covers about 185km by 185km that are taken on two different periods, 31 January 2001 and 5 February 2000 respectively. To carry out image analysis, two scenes were mosaicked and resized to the area of interest. In order to set the correct geographic position of each features, georeferencing of layer stacked Landsat ETM+ bands Band 1, blue (0.45-0.515 μm), band 2, green (0.525-0.605 μm), band 3, red (0.63-0.69 μm), band 4, near-IR (0.75-0.9 μm), band 5, mid-IR (1.55-1.75 μm) and band 7, far-IR (2.09-2.35 μm) with topographic map at the scale 1:50,000 were done by collecting 14 ground control points using nearest neighbour resembling techniques that gives an acceptable RMS value of 0.777. The six spectral bands of the Landsat ETM+ ranges from visible, near-IR and mid-IR regions at a resolution of 30m.

1.5.1.2 Field data

Geological data collection

Geometrical description of dykes, samples of rock and dykes were collected to analyze petrographic description and some samples were sent to France for dating.

1.5.1.3 Software used

The softwares used in this research are as follows:

- ENVI 3.5 was used for georeferencing and different image processing techniques;
- Cartlinx for the digitization and editing of all vector data.
- Arcview 3.2 for data acquisition, analysis and presentation (on screen digitization, grid generation, and overlay analysis);
- AutoCAD Map 2000 for creating 768 grids (2km by 2km) of the area to be used for drainage density calculation and for on screen digitization of contours.

- MapInfo Professional 6 for the purpose of calculating the length of drainage within the grids.
- Microsoft Excel for creating databases for different thematic layers.

1.5.3. Methodology

The flow chart designed below was utilized as a methodology to obtain the desired final out put of the objectives.

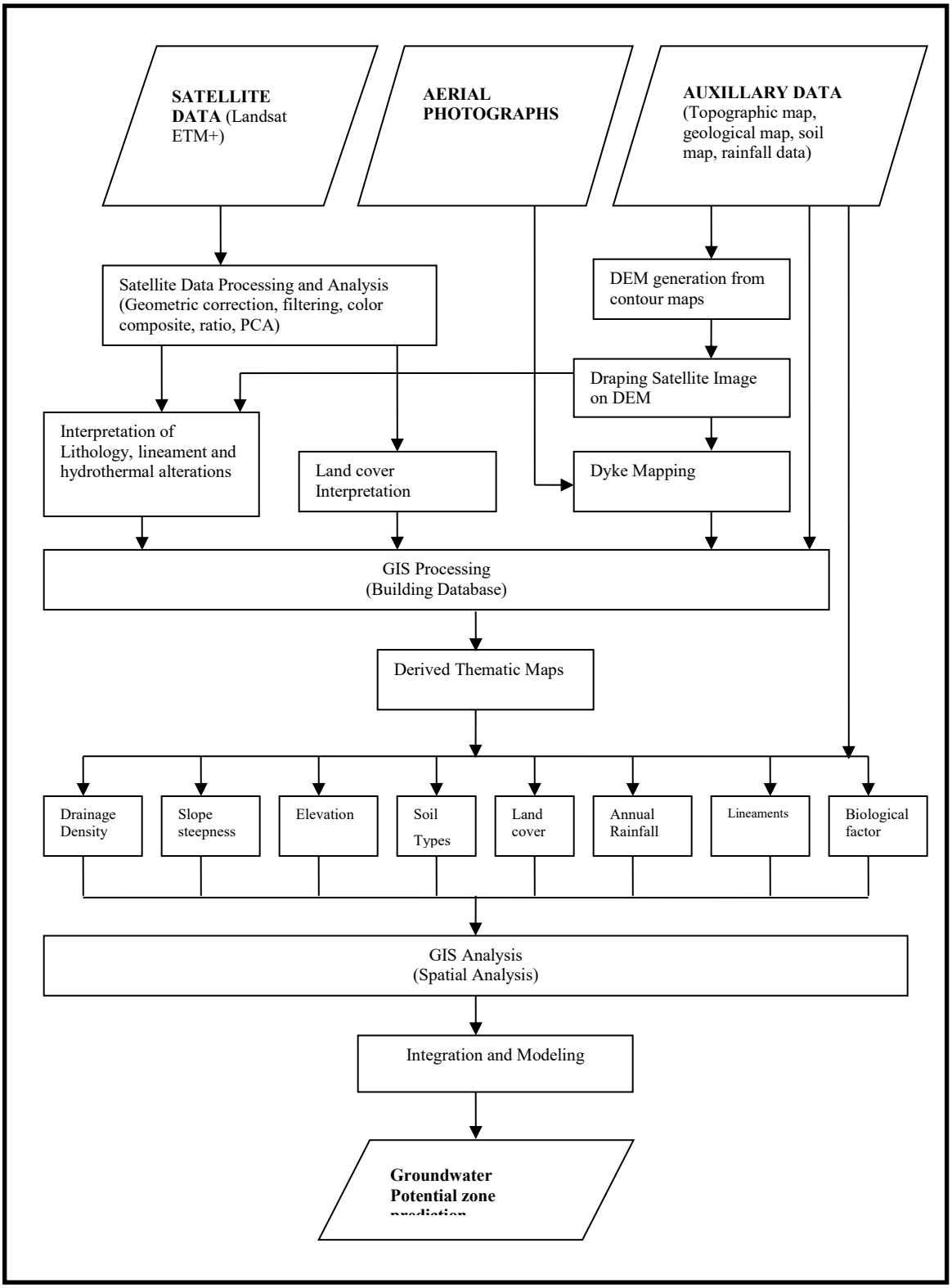

Figure 1.5. Flowchart of the methodology

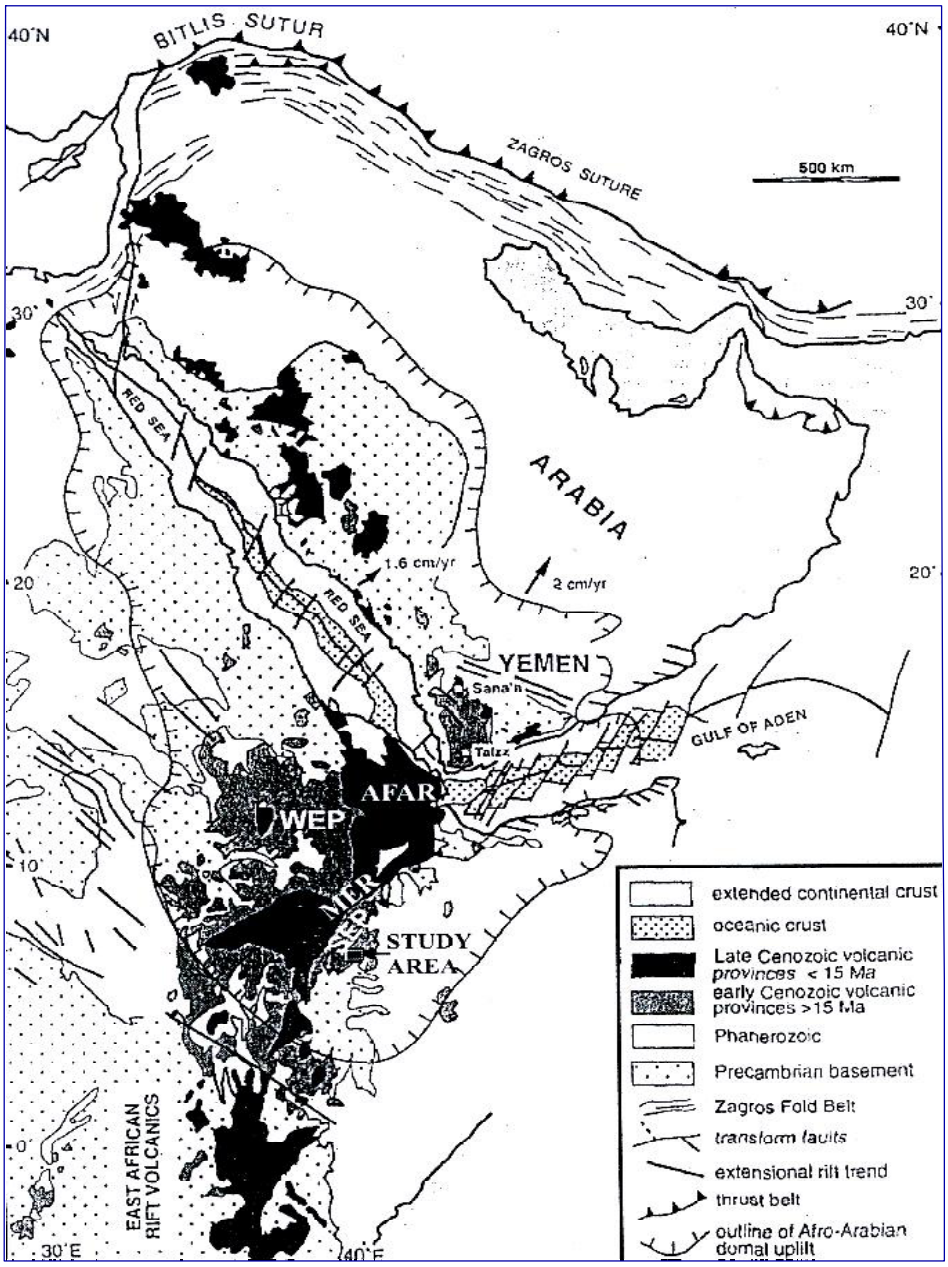

Figure 2.1. Distribution of Cenozoic volcanism in East Africa and Arabian Peninsula after Baker et al. (1996).

The Ethiopian plateau is cut by the Afar and rift valley into two parts, the western and eastern Ethiopian plateau. In SE Ethiopia, the lower stratoid flood basalts range from 30±4.5 to 23.5±4.5Ma.and unconformably overlain by the Reira-Sanetti shield volcanics, which range from c. 15 to c. 2Ma. The unconformity is marked by a paleosol, as are several of the intervals between the major volcanic stages of Ethiopia. (Berhe et al, 1997)

The Ethiopian flood basalts were erupted in three major stages. Stage 1, which is mainly older than 40Ma, is separated from stage 2, 34 to 30Ma for NW Ethiopia and 40 to 30Ma for SW Ethiopia, by erosional unconformities. Stage 3 spans 30 to 26Ma in NW Ethiopia, and 30 to 21Ma in SW Ethiopia and both are marked by the incoming of silicic volcanism. In W Ethiopia, stages 1 and 3 are not developed, whilst in SE Ethiopia the tertiary volcanism commences with stage 3 flood basalts. The overlying shield volcanics; (25 to 13Ma in NW Ethiopia and 15 to 7Ma in W Ethiopia) represent a localized terminal episode built on the plateau and are considered a fourth stage.

The earliest volcanism is restricted two areas: in SW Ethiopia, where the Akobo basalts give ages as old as 49.4Ma (Davidson and Rex 1980), and in NW Ethiopia the Ashenge basalts underlie the Aiba basalts which are dated at 34 to 30Ma.

The Cenozoic volcanism of Bale area, a layer of basalt and trachytes form a thickness of about 2000-2300 m. The Lower Stratoid Basalts, the Reira Basalts, the Dodola and Arorsa Trachytes and the Sanetti Basalts and Batu Trachytes. The Lower Stratoid Basalts, which is the oldest volcanics, is represented by Aiba flood basalts. These are overlain by the Damole Ignimbrites that composed of rhyolites and alkali rhyolites with welded and unwelded ashflow tuffs (Berhe et al, 1987). The silicic lavas and the pyroclastics belonging to the Alaji Formation have no representative in this region. The shield- forming Termaber basalts are represented by the Bale Shield volcanics which are localized and terminal episodes built on the plateau flood volcanics.

There are four major formations of flood volcanic successions that are subdivided based on composition and age. These are:

1. Ashenge flood Basalt Formation,
2. Aiba flood Basalt Formation,
3. Alaji Rhyolite Formation, and
4. Termaber Shield Basalt Formation

The older rock formations cover much of the plateau regions of Ethiopia.

The volcanic successions in Bale area are divided into four groups (Berhe et al, 1987). From the oldest to the youngest are described below:

1. The Lower Stratoid Basalts,
2. The Reira Basalts,
3. Dodola and Aroresa trachytes, and

4. Sanetti Basalts and Batu Trachytes.

1. The Lower Stratoid Basalts

This volcanic rocks, 10m to 150m of thickness, lie on Proterozoic basement rocks. The rock types are dominated by basaltic flows that are weathered and aphyric texture. K-Ar dating shows age range from 30±4.5 to 23.5±4.5Ma (Berhe et al, 1987). This unit is overlain by Damole ignimbrites (200m-250m thick composed of rhyolites and alkali rhyolites with welded and unwelded ashflow tuffs) to the east and by the Reira basalts to the west.

2. The Reira Basalts

It a succession of aphyric, pyroxene and plagioclase-phyric basalts having thickness of 600m. The various units are separated by scoracious basaltic horizons and paleosols. This unit is unconformably overlie the Damole Ignimbrites to the east and the Stratoid Basalts to the west. The Reira basalts have been dated as middle to upper Miocene (5.3±1Ma) (Berhe et al, 1987) and unconformably overlain by Aroresa Trachytes and Dodola Ignimbrites.

3. Dodola and Aroresa Trachytes

This group of rocks consists of rhyolitic ignimbrites, trachytes and ash flow tuffs, with fluvio-lacusterine intercalations within the ignimbrites. The rocks are restricted to the Dodola area and are unconformably underlain by the Reira basalts. These units are of upper Miocene to Pliocene (5.3-2.1 Ma). These volcanics were described by Merla et al, 1979 as the Ginir Unit to which were ascribed age of 6 to 2Ma. The Dodola ignimbrite is named separately as the Adaba Ignimbrite of age 2.35 Ma. (Eberz et al. 1988).

4. Sanetti Basalts and Batu Trachytes

This forms the second volcanic edifices in Ethiopia. These volcanics were erupted from different centres show rapid lateral thickness variations. Frequently recent olivine basalts are observed along riverbeds, in a few cases covering tens of kilometres. These rocks are dated as late Pliocene (2 Ma, Sanetti basalts) to Quaternary (Batu Trachytes).

2.2. Field observations

At the central part of the study area there are huge trachytic and rhyolitic lavas that flow towards west and north from their sources. The sources of the lava flows looks like coming from central vents aligned along a given structure (elongated fissure). Satellite image interpretation shows the presence of major NE-SW structure along the source of the lava. There are NE-SW aligned rivers that are indicative of pre-existing tectonic event. The evidence of succession of volcanic products of Ash, Ignimbrite flow and Trachytic lava are typical exposures around central volcano. The presence of trachytic plugs is also indicative of central volcanic activities on the area. The sense of flow of the lava looks like as it come out from a given centre and expands away from the centre.

Due to regional coverage capability satellite image, caldera feature was identified. It shows tilting blocks around the rim of the caldera (Figure 2.2.). The caldera is ~16 km by ~13 km in diameter. Post caldera volcanic activities are observed inside the caldera as interpreted from images.

The presence of recent mafic scoracious basalt, the presence of normal faults morphology which are not well matured and the presence of elongated structure (fissure) where recent lava flows come out through vents possibly show the area is still geologically active. Unlike rift valley, where there are regional extensions, the Bale Mountains and the surrounding area does not show well defined tectonics.

Figure 2.2. Tilting blocks on the rim of the caldera.

CHAPTER 3: Application of remote sensing in geological investigation

Geological mapping involves recording geological information on to a map. The geological information includes the distribution, nature and age relationships of the rock units and the occurrence of structural feature, mineral deposits (Jackson 1997). Since conventional geological mapping involves men working in the field and logistics, it is time, cost and effort consuming work. In contrast, remote sensing images that cover large area with in short time and low cost is usually used for geological explorations before conducting field works. Remote sensing sensors can detect different reflectance beyond human eye can detect that is limited to the visible portion of electromagnetic spectrum.

Areas covered by vegetation and/or weathering product, the images obtained from these covers are not representative of the bedrock geology. On the other hand different bedrocks support different vegetation, and different bedrocks produce different alterations. This shows that it is possible to indirectly reflect the characteristics of the bedrock, therefore it is used to support geological mappings. In addition to geological mapping, hydrothermal alterations that are related to certain mineral deposits can be well mapped Sabins, (1999). The six spectral bands of the Landsat ETM+ at visible, near-IR and mid-IR regions at a resolution of 30m were considered for this purpose. Landsat ETM+ bands are (Band 1, blue (0.45-0.515 μm), band 2, green (0.525-0.605 μm), band 3, red (0.63-0.69 μm), band 4, near-IR (0.75-0.9 μm), band 5, mid-IR (1.55-1.75 μm) and band 7, far-IR (2.09-2.35 μm) (Figure 3.1). Here an attempt was made to identify features (geologic or landcover) using remote sensing image interpretation.

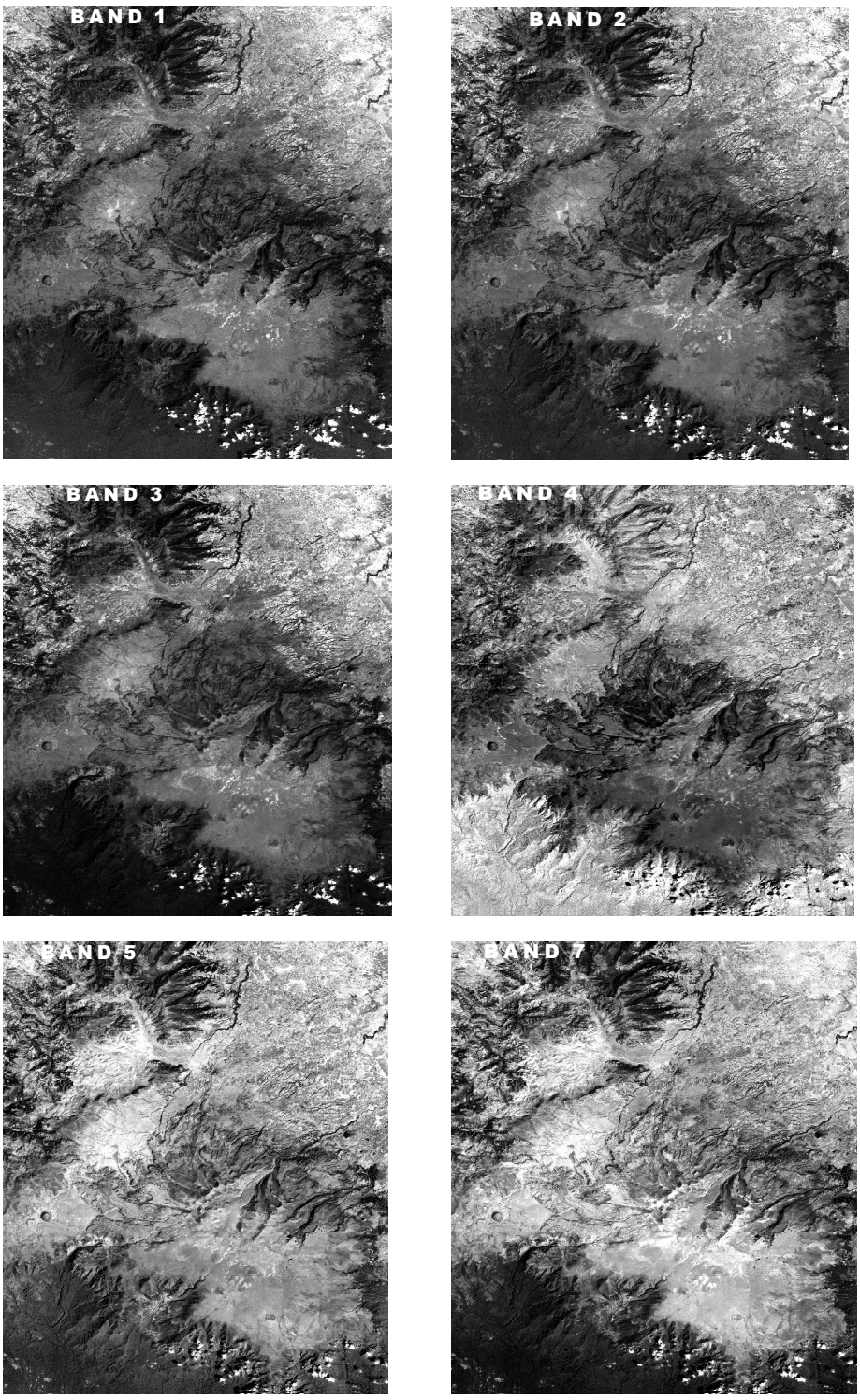

Figure 3.1 Landsat ETM+ bands, band 1,2,3,4,5, and 7 of the study area.

3.1 Ratio images

Remote sensing softwares help to analyze the mineral content of an area from the Landsat images. Figure 3.3 shows laboratory reflectance of iron oxides and clay minerals that is the basis for ratio analysis. The three ratios, 3/1, 5/7, and 5/4 were selected for their sensitivity to lithologic variables and for their lack of statistical redundancy (Crippen, 1989, Crippen et al., 1988). Iron oxides have high reflectance at Band 3 and low reflectance at Band 1 of the Landsat images (Figure 3.4 A.). Ferrous minerals have high reflectance on the ratio of band 5 and band 4 (5/4) (Figure 3.4.B). Clay minerals and vegetation have high reflectance at Band 5 and significantly lower reflectance at Band 7 (Figure 3.4.C). The ratios, Band 5/Band 7 for vegetation and clay minerals, Band 5/Band 4 ratio for ferrous minerals, Band 3/Band 1 ratio for iron oxides (ferric iron), and color composite of the three ratios were tested on the study area.

As it is clearly observed the deep blue colour on (Figure 3.4 D) may be misinterpreted as clay rich terrain, but it is vegetation. This is because clay minerals and vegetation characterize high reflectance on ratio image of band 5 and band 7. To separate the clay and vegetation area ratio of band 4 and band 3 were tested due to the reason that the reflectance of vegetation is higher on this ratio than band 5 and band 7 but it was difficult to distinguish them.

Color composite of the ratio bands 3/1, 5/4 and 5/7 clearly identified the vegetated area and the rocky terrain. As it is observed on (Figure 3.4 D) southern and northern central part of the area is well-vegetated area as depicted from its blue color in response to high reflectance of vegetation on band 5/7. The Sanetti plateau entirely covered by volcanic products show high response for ferrous and ferric iron content and appears as variation of green and red. On the Sanetti plateau the ferrous minerals appears the dominant geochemical composition especially on the intermediate (Trachytic lava flow) and acidic (rhyolitic lava flow) that flows towards western and northern part of the Sanetti plateau.

Further enhancement of the hybrid colour composite 3/1, 5/4, 5/7 (RGB) transformed into the HLS (hue, lightness, saturation) identify distinct geologic unit in the vegetated area. (Figure 3.5). On the 1:250000 geological map, only one intrusive syenite exposure is mapped as Hornblende alkali-feldspar syenite and lesser Hornblende nepheline syenite that intruded aphyric and porphyritic basalt.

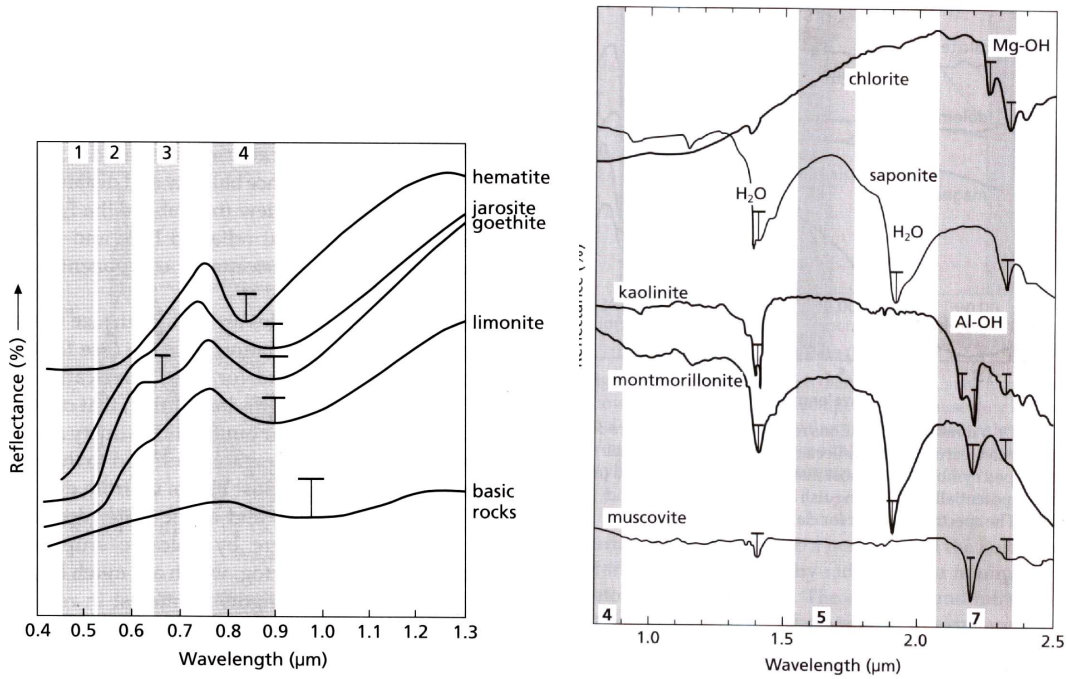

Figure 3.3. Laboratory reflectance spectra for iron oxides and clay minerals (Drury, 2001)

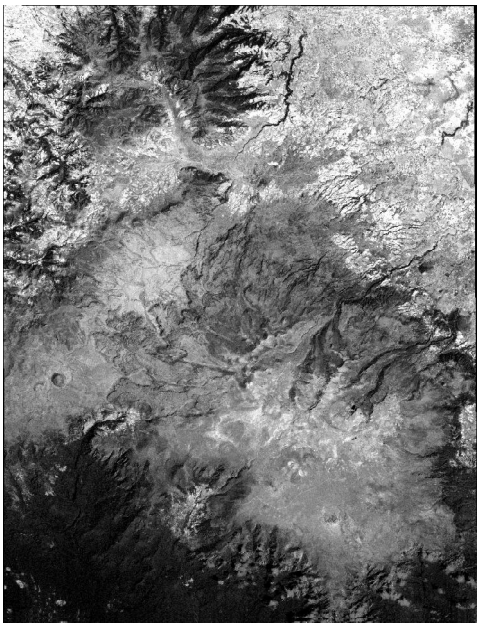

A= Ratio:(3/1)

B= Ratio:(5/4)

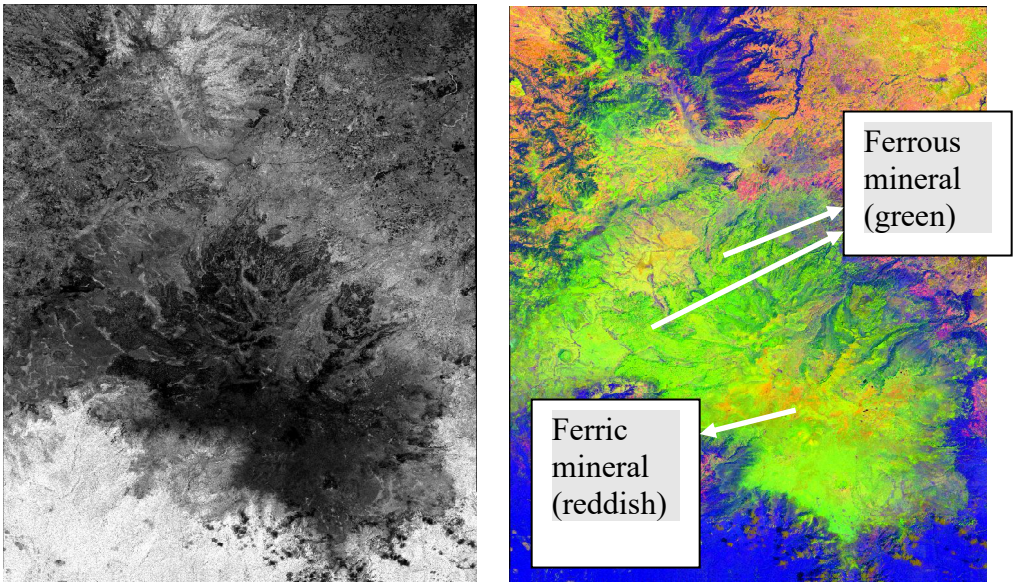

C=Ratio:(5/7) **D**=3/1, 5/4, 5/7 (RGB)

Figure 3.4 Ratio images and their colour composite 3/1, 5/4, 5/7 (RGB)

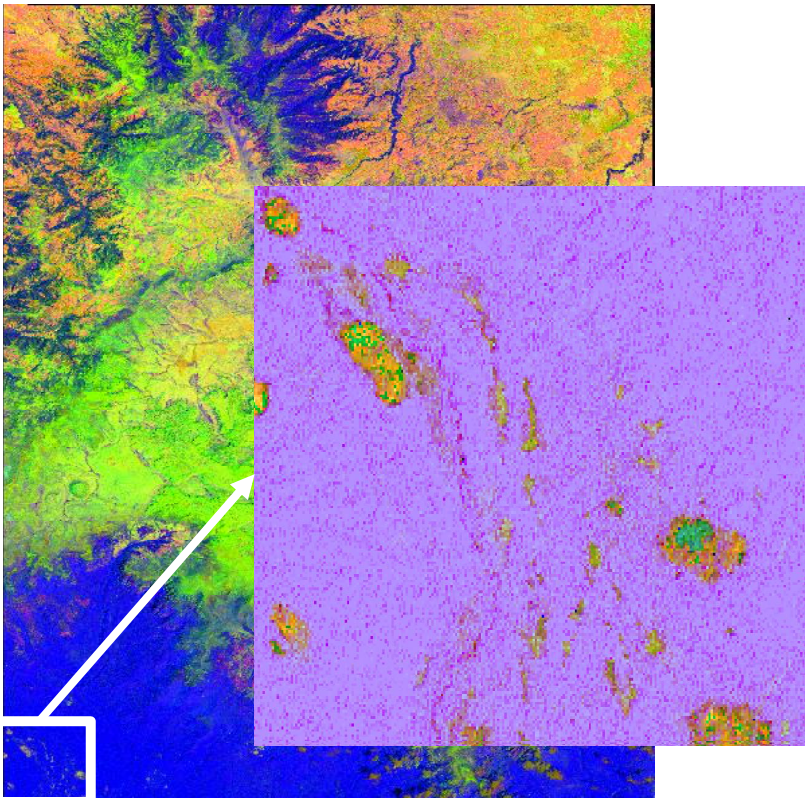

Figure 3.5 Ratio color composite 3/1, 5/4, 5/7 (RGB) transformed into the HLS (hue, light and saturation), the syenite rock is clearly identified within forest.

3.2 Principal component analysis

The application of principal component analysis on geological investigation is a means of concentrating important information about earth features into a few principal component images. The analysis generates the same number principal components as the number of bands used. The first principal component contains the highest variance from all bands used. As the order of the principal component increases the information contents will decrease. The principal component images are expressed by Eigen vectors, which are the loadings of each band to highlight spectral variation between the principal components. The loadings are high and positive for the first principal component indicating that the first PC is the average of all bands involved in the principal component analysis. Principal component analysis is a means of data reduction by compressing the original data into a lower order component. The principal components can be displayed as false colour composite image. The decolrrelation between different principal components allow subtle variation of surface features. Based on these assumptions principal component analysis were tested for the study area. The available ETM+ bands 1, 2, 3, 4, 5 and 7 grouped into band 1, 3, 4 and 5 and bands 1, 4, 5 and 7 due to their sensitivity for ferric minerals and OH^- containing minerals respectively. Principal component with high positive or negative loadings for band 1 and band 3 in the eigenvector matrix gives a measure of redness that is related to oxidized iron minerals. Likewise, principal component of OH^- will similarly have high loadings for bands 5 and 7 in the eigenvector matrix. By adding these two PCs will give the third PC which highlight areas rich in iron oxides and/or OH^- (Drury, 2001).

1. PCs for bands 1, 3, 4, and 5 (Table 3.1.)

Eigenvectors

PCs	Band 1	Band 3	Band 4	Band 5
PC1	0.624725	-0.372918	0.562078	0.393342
PC2	0.068720	0.215905	0.602442	-0.765327
PC3	-0.270142	-0.901720	-0.066425	-0.330927
PC4	-0.729396	0.034902	0.562778	0.387354

Table 3.1. PCs for bands 1, 3, 4, and 5

Interpretation of statistics of the above eigenvector matrix shows that the eigenvector for PC 1 shows high degree of variability of loading from band 1 having positive eigenvector in contrast to

negative loading of band 3 (Figure 3.6 A). PC 1 is considered to detect ferric minerals. A component that has high positive loading on band 4 and high value with negative loading band 5, expresses the vegetation density and variability (Figure 3.6B) shows distinct bright feature of vegetation). PC 4 shows high positive and negative loading between band 1 and band 5 that show the presence of clay containing soil. PC 3 lacks to show any peculiar feature as a reason it is omitted to be incorporated in the false color composite (Figure 3.6 D). Figure 3.7 shows PC 1, PC 2, PC 3 displayed as (RGB) that distinctly identify the vegetated area, the clay containing soil and ferric rich volcanic materials.

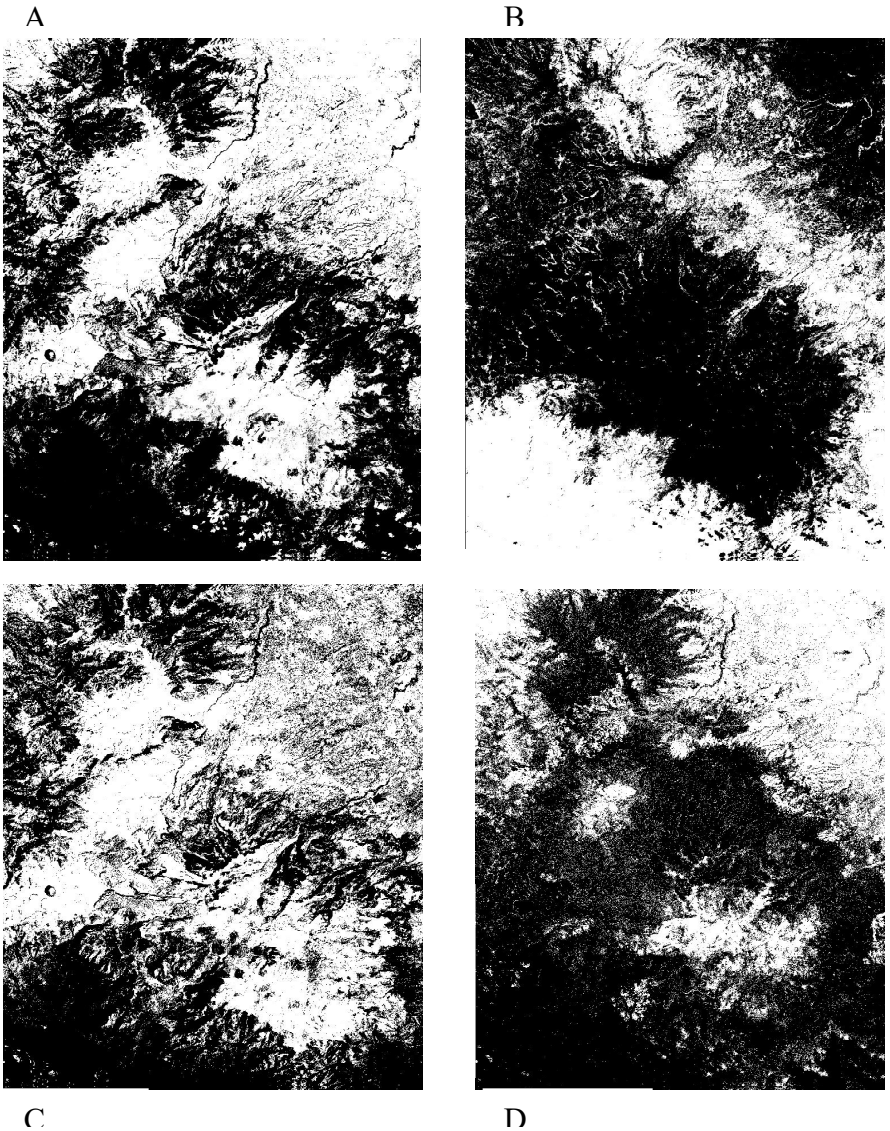

Figure 3.6. Principal component images derived from bands 1, 3, 4, and 5 (A, B, C, D)

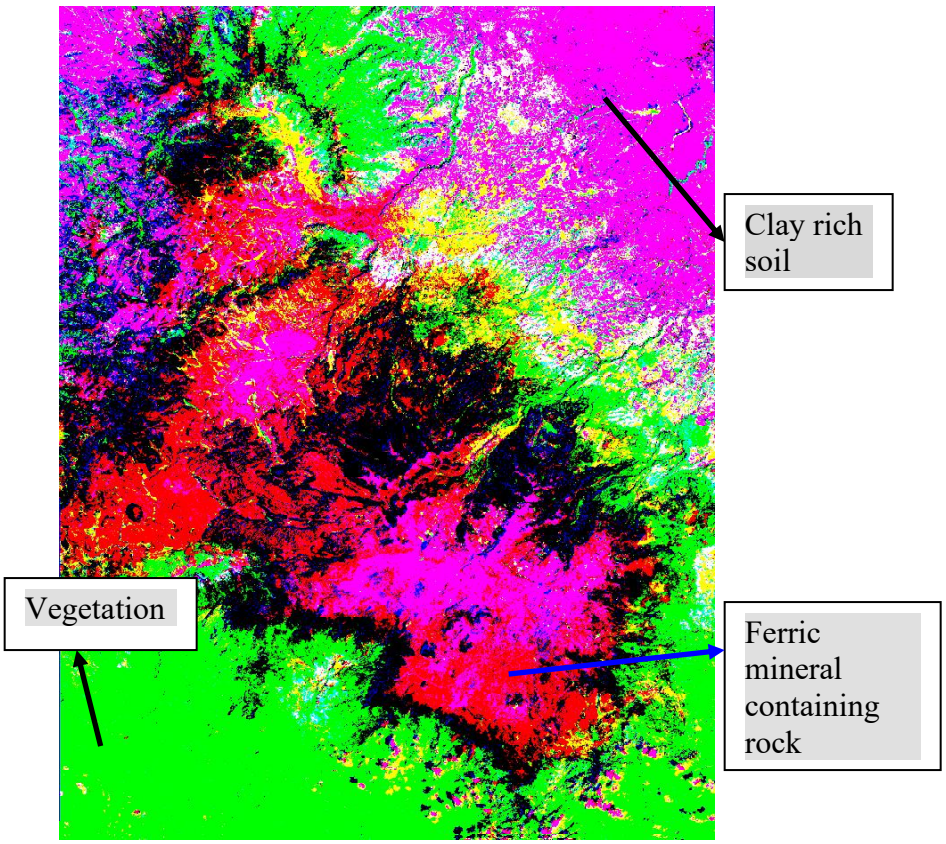

Figure 3.7. PC1, PC2, PC3 displayed as false colour composite in (RGB).

For the analysis of principal components derived from band 1, 4, 5 and 7 the following eigenvectors table were generated (Table 3.2) and interpreted the similar way as interpreted for PCs generated from band 1,3,4 and 5.

Eigenvectors

PCs	Band 1	Band 4	Band 5	Band 7
PC1	-0.602730	0.279841	0.613901	0.426065
PC2	-0.090386	0.782247	-0.017715	-0.616122
PC3	0.413096	0.556399	-0.302301	0.654512
PC4	0.676682	0.014079	0.728990	-0.102356

Table 3.2 PCs for band 1, 4, 5, and 7

PC 1 enhances the rocky surfaces (band 7 has high sensitivity for rocky surface); PC 2 and PC 3 enhance the vegetated area (high positive loading of band 4). PC 4 has high loading for from band 5 and negative loading from band 7 that may imply the presence of clay.

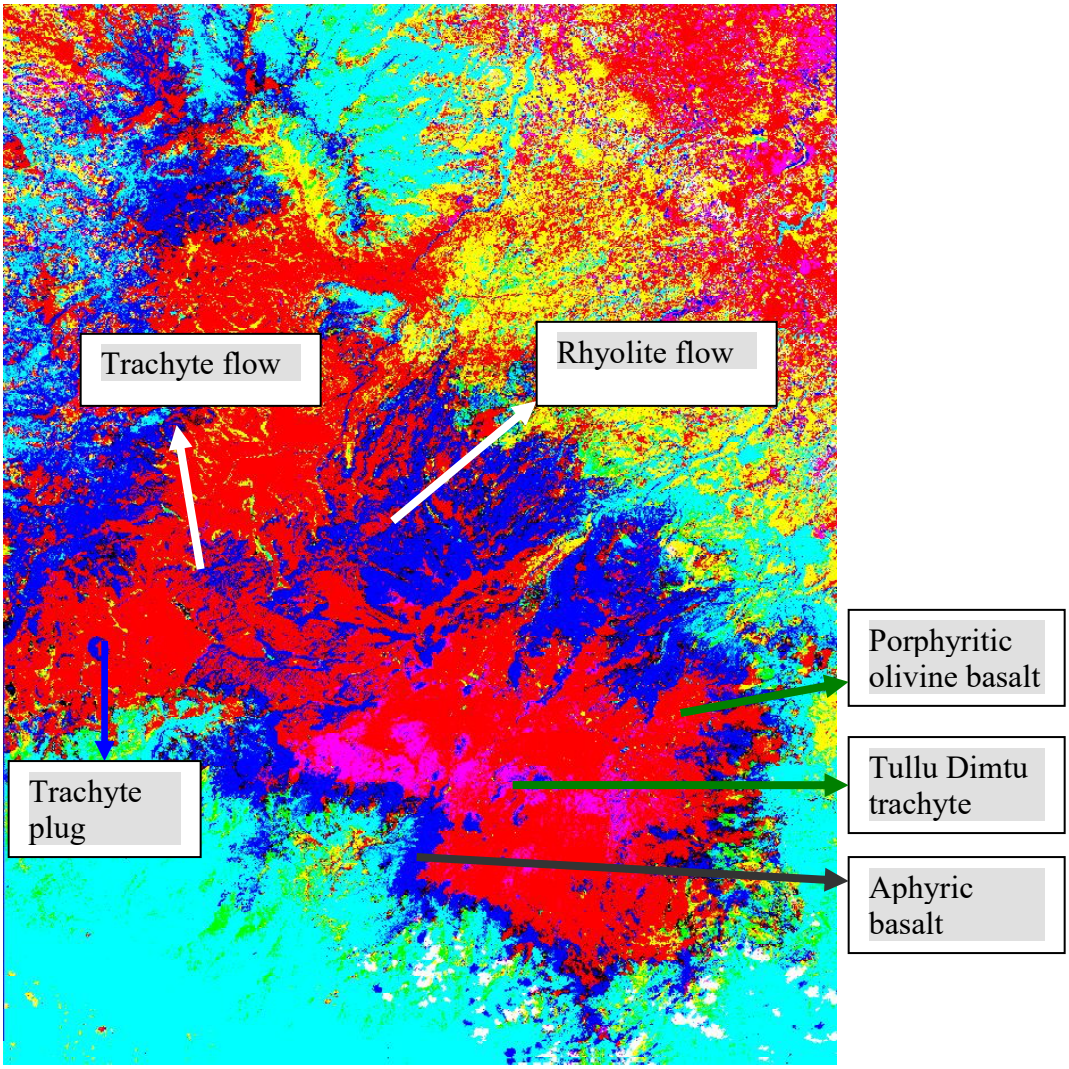

Figure 3.8 Principal component color composite image PC1, PC2, PC3 (RGB) derived from Principal component analysis of band 1, 3, 5 and 7.

Different rock types can have similar reflectance; trachyte and/or Rhyolite, and basalt show similar reflectance depending on the surface smoothness. As shown on the PC color composites image, both rock types have red color at places where the surface smoothness is similar. The sanetti plateau is mainly basaltic volcanic material that is also evidenced from petrographic analysis- e.g. porphyritic olivine basalt (see Table 3.3 petrographic analysis San-2). The blue color represents intermediate and acidic materials-trachyte and rhyolite. The blue color at SW part of the image, on the eroded (rough surface) Harenna escarpment represents Aphyric basalt.

Therefore, It can be concluded that smooth areas within the trachyte and rhyolite rocks appears red in color as the basalt on the sanetti plateau.

From Table 3.1 PC1 (detecting ferric mineral) and from Table 3.2 PC4 (detecting clay mineral) were tested to enhance the sensitivity of ferric mineral and/or OH^- . This is done by adding PC1, PC4, then displaying PC1, PC2 and PC1+PC4 as (RGB). The resultant image is shown below (Figure 3.9). It shows similar regions like the images interpreted above

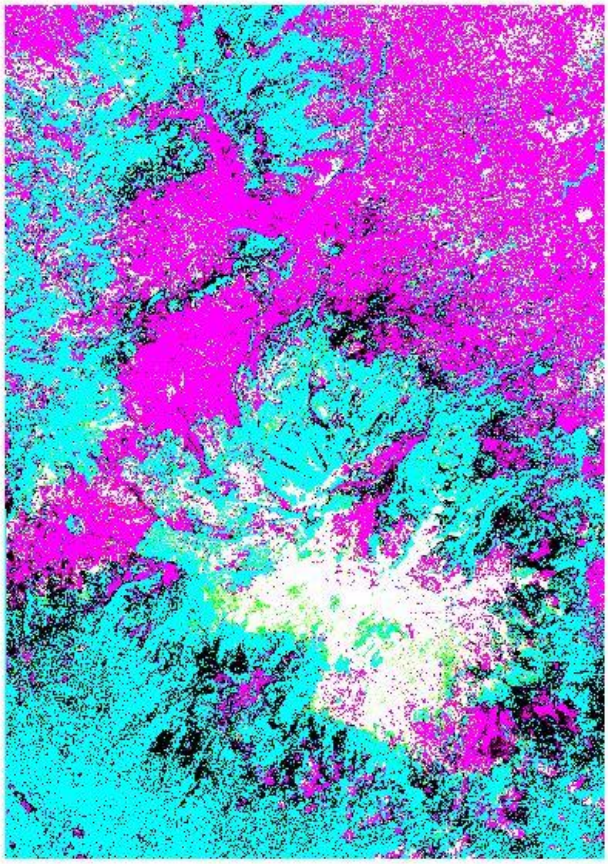

Figure 3.9 Color composite images of PC1, PC4, PC1+PC4 (RGB)

Generally it can not be totally rely on remote sensing for geologic mapping because as shown in the study area the vegetation cover hinders information that can be obtained from rocks and similar reflectance can be recorded due to compositional similarities of rocks e.g. Trachyte and Rhyolite.

CHAPTER 4: Dyke analysis

4.1 Regional distribution of dykes in Ethiopia

On the rift margin, the Sagetu Ridge dyke swarm has been studied by Mohr and Potter (1976), Mohr (1980), and kennan et al., (1990). On the western Ethiopian plateau, the best known dyke swarm exposures are on the Afar margins and the plain area southwest of Lake Tana, Dykes exposed across the tilted blocks of the Afar margin along the Kombolcha-Bati road were investigated by Abate and Sagri (1969), Justin-Visentin and Zanettin (1974), and Mohr (1983). Reconnaissance mapping of dykes in Tana-Belaya area, western Ethiopia, has been carried out by Jepsen and Athearn (1963a). In Tana Belaya area field investigation and satellite image analysis shows the existence of two dyke swarms, the NE-SW Serpent-God dyke swarm, and the NW-SE Dinder-dyke swarm having age of 30Ma, is believed to be feeders of the Traps (Mege et al. 2004). Other investigated dyke swarms in Ethiopia and Eritrea include the dykes from the Angareb ring complex (Hahn et al. 1977) and the Asmara dyke swarm (Mohr, 1999). Other dyke swarms have been identified (Mohr, 1971; Mohr and Zanettin, 1988, and personal observations). (Figure 4.1)

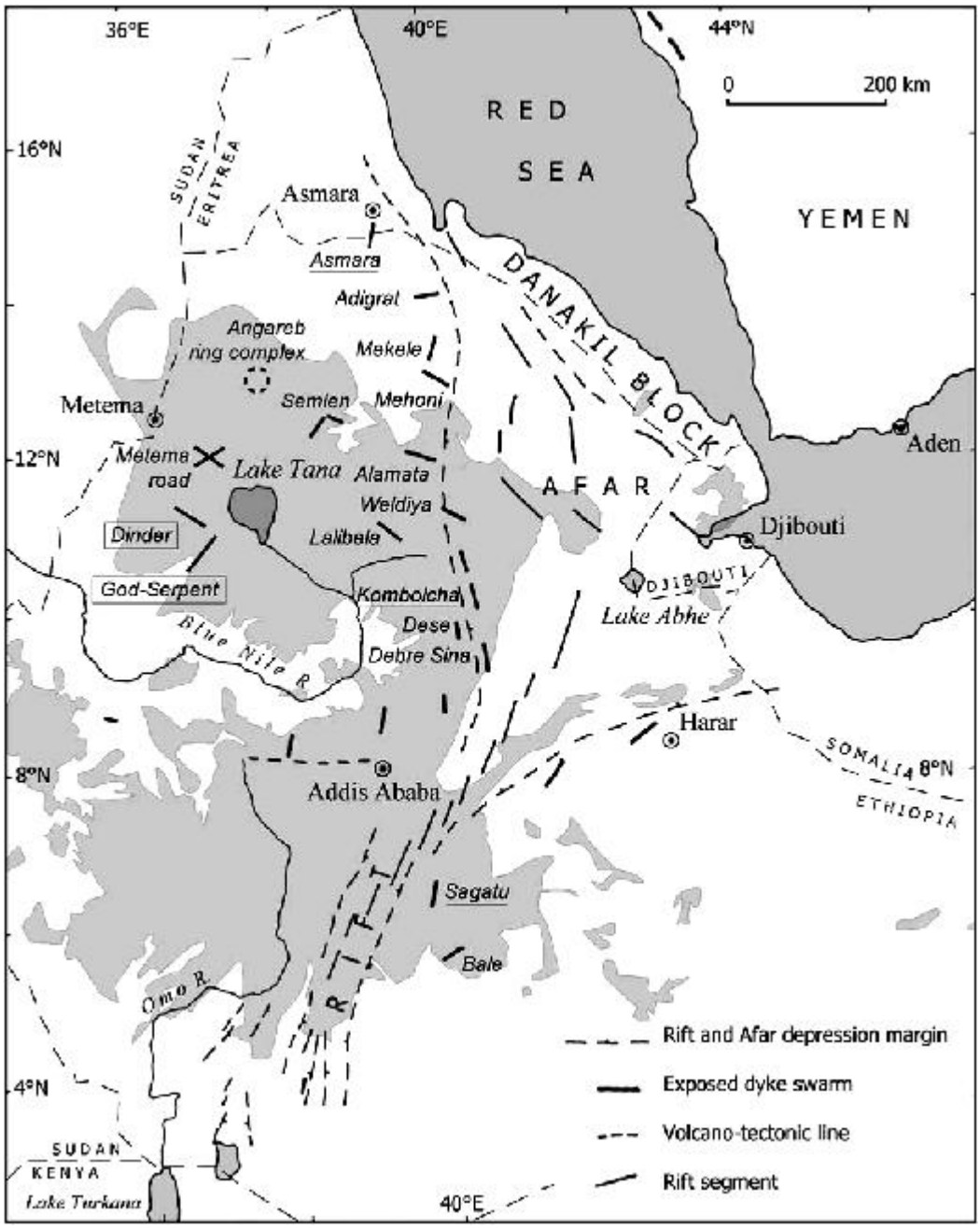

Figure 4.1 Distribution of the main dyke swarms in Ethiopia according to and Modified after Mohr and Zanettin (1988). Many of the dyke swarms except some have not studied yet and unreported swarms may exist.

4.2 Dykes of Bale Mountains and the surrounding areas

Dyke swarms of the Bale Mountains and the surrounding areas have not yet been investigated with regard to their structural and geometrical aspect. Measurements of dip, strike, thickness and composition were taken in the field mainly from the northern part of the study area, called Atiba or Kawa. About 43 dykes were identified on the field that are localized on Kawa area. Due to the problem of inaccessibility it was difficult to identify the likely occurrence of more dykes on the Harenna escarpment and Sanetti plateau. At the southern end of sanetti plateau where the Harenna escarpment starts dykes where observed from the interpretation satellite images. It may imply that there would be many basaltic dykes that likely act as feeders for flood basalt. Age analysis on the dykes and the flood basalt could be a confirmation whether they are a feeder or not. Basaltic dyke exposures may be covered by the thick Harenna forest or not exposed to the surface due to high viscosity of the magma.

Majority of the silicic and mafic dykes are oriented NS and some NE-SW direction (Figure 4.2 and 4.3). In addition, it is observed that EW trending fresh basaltic dyke crossing the older one (Figure 4.4). The dyke strikes are consistent with the strike measured from satellite image and aerial photograph.

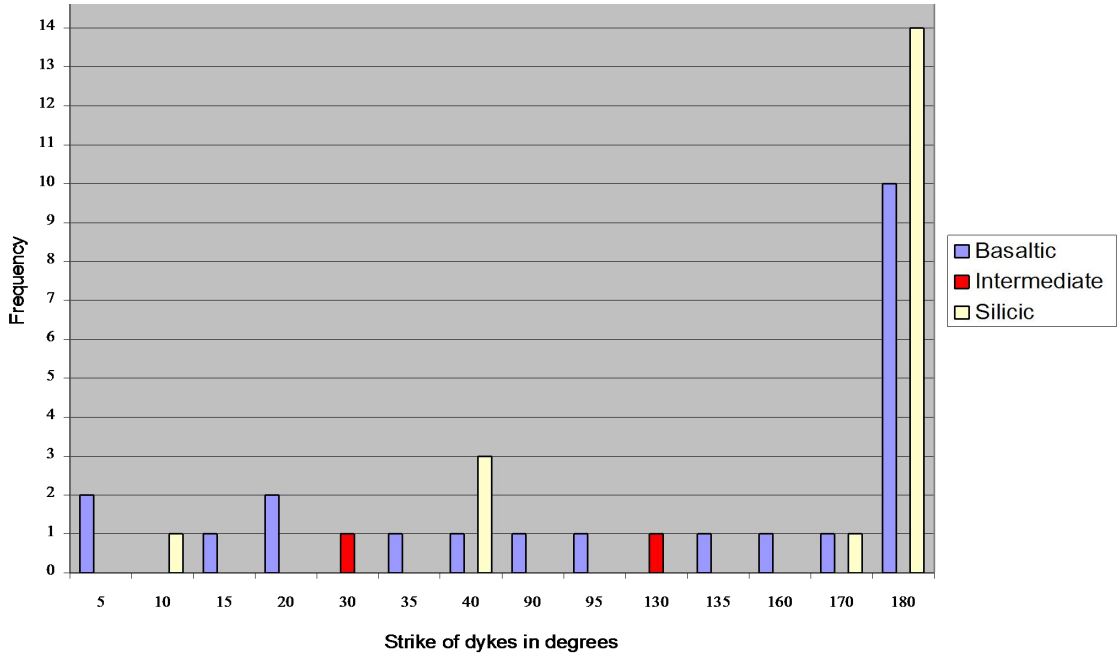

Figure 4.2 Histogram of strike of dykes as a function of compositional variation and frequency for 43 dykes measured in the field.

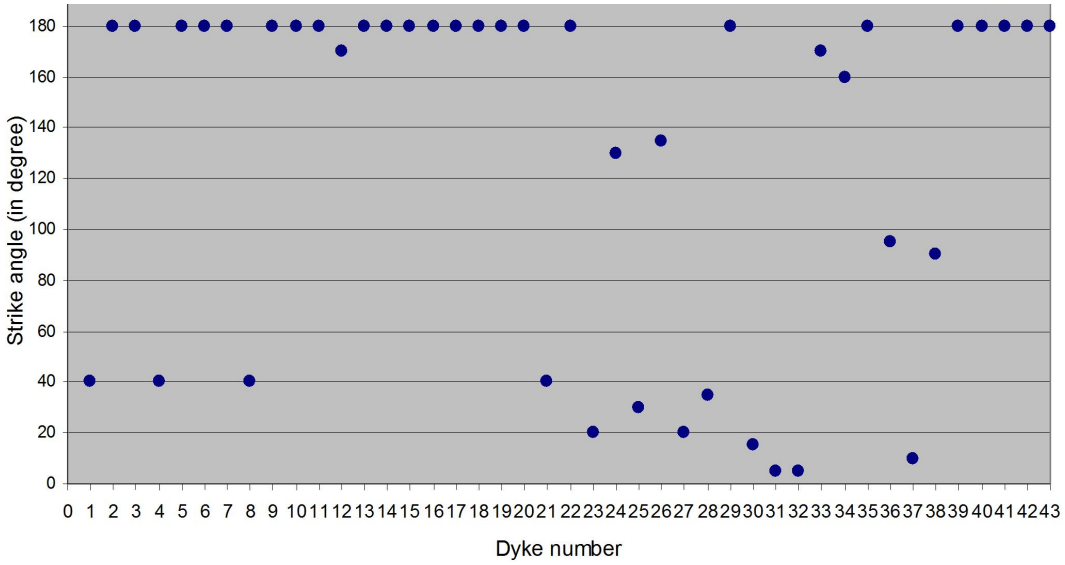

Figure 4.3 Scatter plot of strike angle of 43-dyke measured in the field.

Figure 4.4 Basaltic dykes around Kawa area, where fresh basaltic dyke (injection 2) cross cut the other older basaltic dyke (injection 1).

The dip of the dykes ranges from 45^{O}W-85^{O}W, out of 8 field measurements, 7 dykes are basaltic and only 1 dyke is silicic in composition. All dykes have dipping towards west; most of them have dip between 75^{O} and 85^{O} (Figure 4.5)

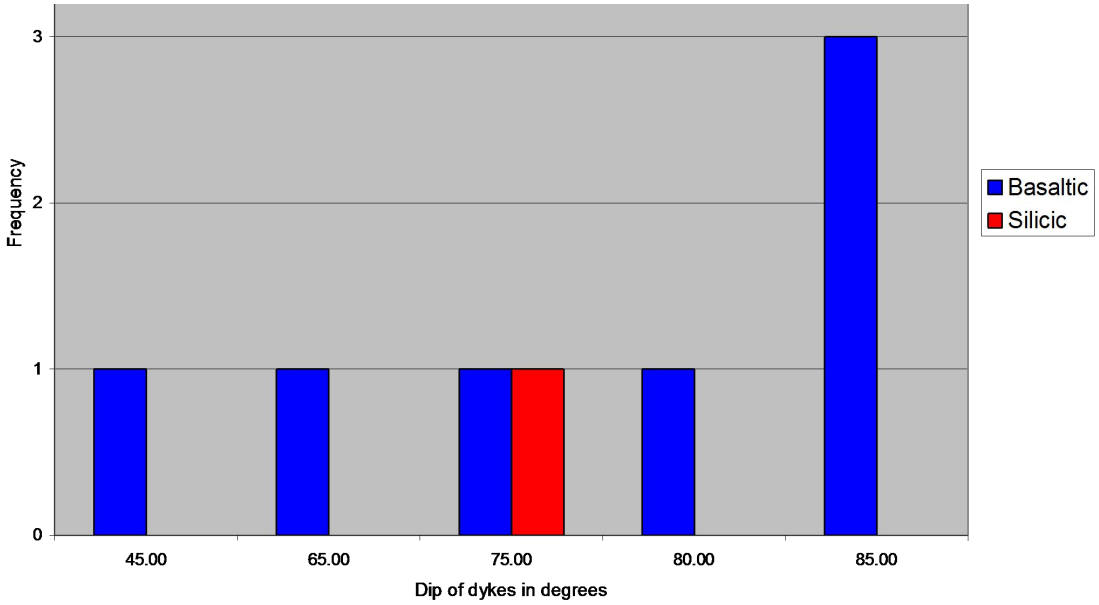

Figure 4.5 Histogram of dip of dykes measured in the field as a function of compositional variation and frequency.

Majority of the dykes have thickness (surfacial cover measurement) less than 10m (Figure 4.6.). During field observation only two dykes have a thickness of about 20m and 25m.

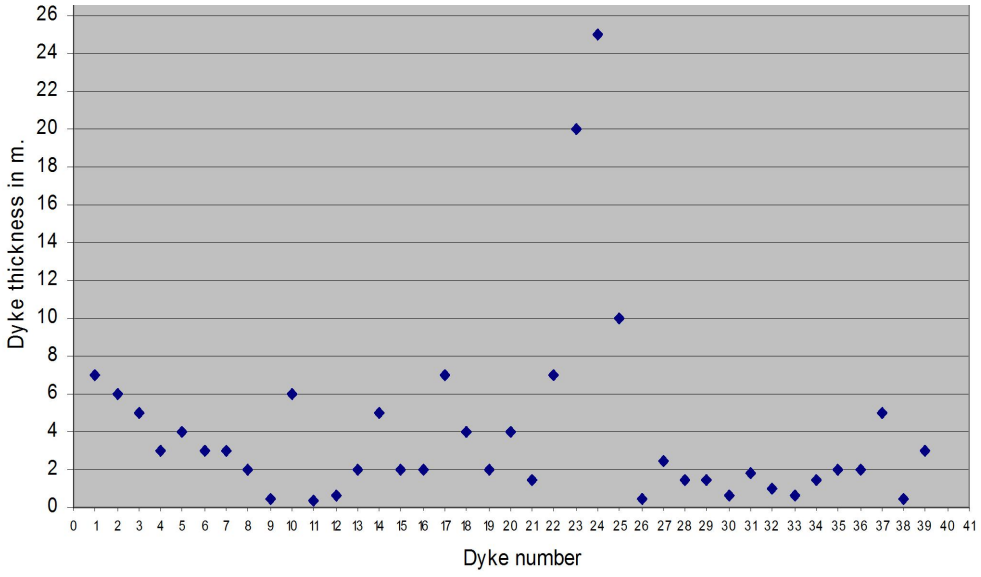

Figure 4.6 Scatter plot of 43-dyke thickness measured in the field.

Satellite interpretation of the Landsat ETM+ image was not spatially detailed enough to identify the short thickness and length of dykes on the Bale Mountains and the surrounding areas. Short

length of the dykes can be interpreted, as due to local tectonics, otherwise the dykes must have kilometres of length if it is related to regional tectonics. High viscosity of the silicic dykes creates vertical topographic relief for these dykes than basaltic dyke and is more easily identifiable on the field and aerial photograph. Some of the silicic dykes on Kawa area show en echelon arrangement.

Around Kawa the composition of the dykes is variable ranging from mafic, intermediate to acidic (majority). It may imply the area is the center of volcanism. It is also evidenced that there are N15^{O}E, N5^{O}E, N170^{O}E dykes oriented that looks radiating from a given center (Figure 4.7). The basaltic rocks and dykes exposed at Kawa area have porphyritic texture was showing the presence of shallow magma chamber that allow the crystals to grow at a bigger size.

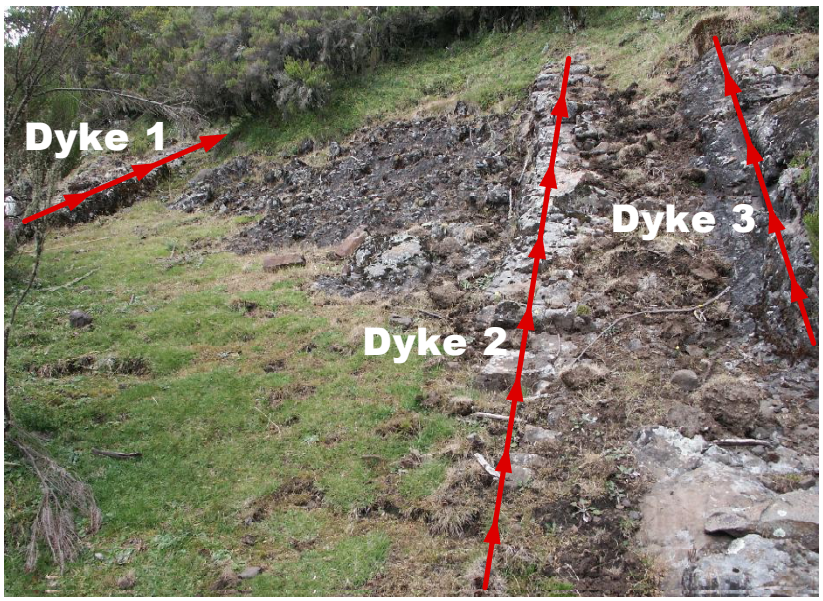

Figure 4.7 Radiating dykes around northern part of the study area (Kawa).

During fieldwork springs have been observed emerging out through fractures at the contact between the country rock and basaltic dykes, and between the valley and the dyke (Figure 4.8). These could be the effect of local groundwater movement. Unlike the mafic dykes the silicic dykes do not show baked and chilled margin (Figure 4.9a and Figure 4.9b)

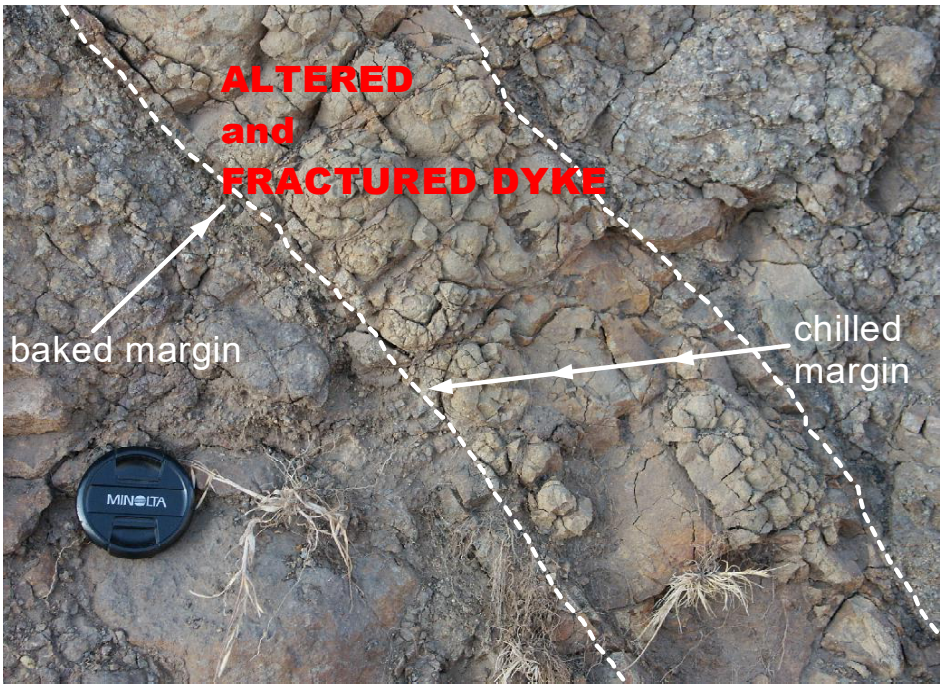

Figure 4.8 Altered and fractured dyke with chilled and baked margin.

Figure 4.9a Silicic dyke not showing chilled and baked margin.

Figure 4.9b Field photograph of columnar jointing due to cooling effect on Basaltic dyke; strike N5^{O}E, thickness 1.8 m. Water comes out at the contact of dyke and country rock

Though the trend of the dykes is similar to those found in the main Ethiopian rift and the Sagetu ridge dyke, the dykes on Bale Mountain and the surrounding area are smaller both in thickness and length so that it may imply local tectonic effect.

The silicic dykes are sub-vertical and the ς_3 the direction of the minimum compressive principal stress is horizontal and perpendicular to trend of these dykes. During dyke emplacement, the minimum principal compressive stress was therefore mostly trending EW. Table 4.1 below shows measurements of different parameters measured in the field and figure 4.10 shows mapped dykes, faults, lineaments and thin section sample locations.

Dyke number	Easting	Northing	Thickness	Strike	Composition	Dipping
1	564996	778909	7.0	40	Silicic	
2	576570	796438	6.0	180	Silicic	
3	576543	796437	5.0	180	Silicic	
4	576525	796417	3.0	40	Silicic	
5	576543	796378	4.0	180	Silicic	
6	576500	796378	3.0	180	Silicic	
7	576434	796353	3.0	180	Silicic	
8	576429	796353	2.0	40	Silicic	
9	576903	796493	0.5	180	Silicic	
10	576849	796469	6.0	180	Silicic	
11	576852	796508	0.4	180	Basaltic	
12	576840	796503	0.6	170	Silicic	
13	576632	796658	2.0	180	Silicic	
14	576961	796890	5.0	180	Silicic	
15	576950	796992	2.0	180	Basaltic	85
16	576848	797066	2.0	180	Silicic	
17	576590	796993	7.0	180	Silicic	
18	576723	796970	4.0	180	Silicic	
19	576330	797052	2.0	180	Basaltic	
20	576330	796878	4.0	180	Silicic	
21	576208	796628	1.5	40	Basaltic	75
22	576279	796520	7.0	180	Basaltic	
23	567978	779222	20.0	20	Basaltic	
24	568402	779337	25.0	130	Intermediate	
25	590847	753703	10.0	30	Intermediate	
26	577521	797151	0.5	135	Basaltic	
27	577569	797577	2.5	20	Basaltic	85

28	577569	797577	1.5	35	Basaltic	
29	577569	797577	1.5	180	Basaltic	
30	577532	797686	0.6	15	Basaltic	
31	577532	797686	1.8	5	Basaltic	
32	577532	797686	1.0	5	Basaltic	
33	577532	797686	0.6	170	Basaltic	
34	577532	797851	1.5	160	Basaltic to Intermediate	
35	577570	797249	2.0	180	Basaltic	65
36	577580	797402	2.0	95	Basaltic	
37	577315	797965	5.0	10	Silicic	75
38	576901	797982	0.5	90	Basaltic	
39	576889	797980	3.0	180	Basaltic	45
40	576839	797969		180	Basaltic	
41	576845	797990		180	Basaltic	85
42	576793	797943		180	Basaltic	80
43	576534	797693		180	Silicic	

Table 4.1. Geometric measurements and composition of dykes.

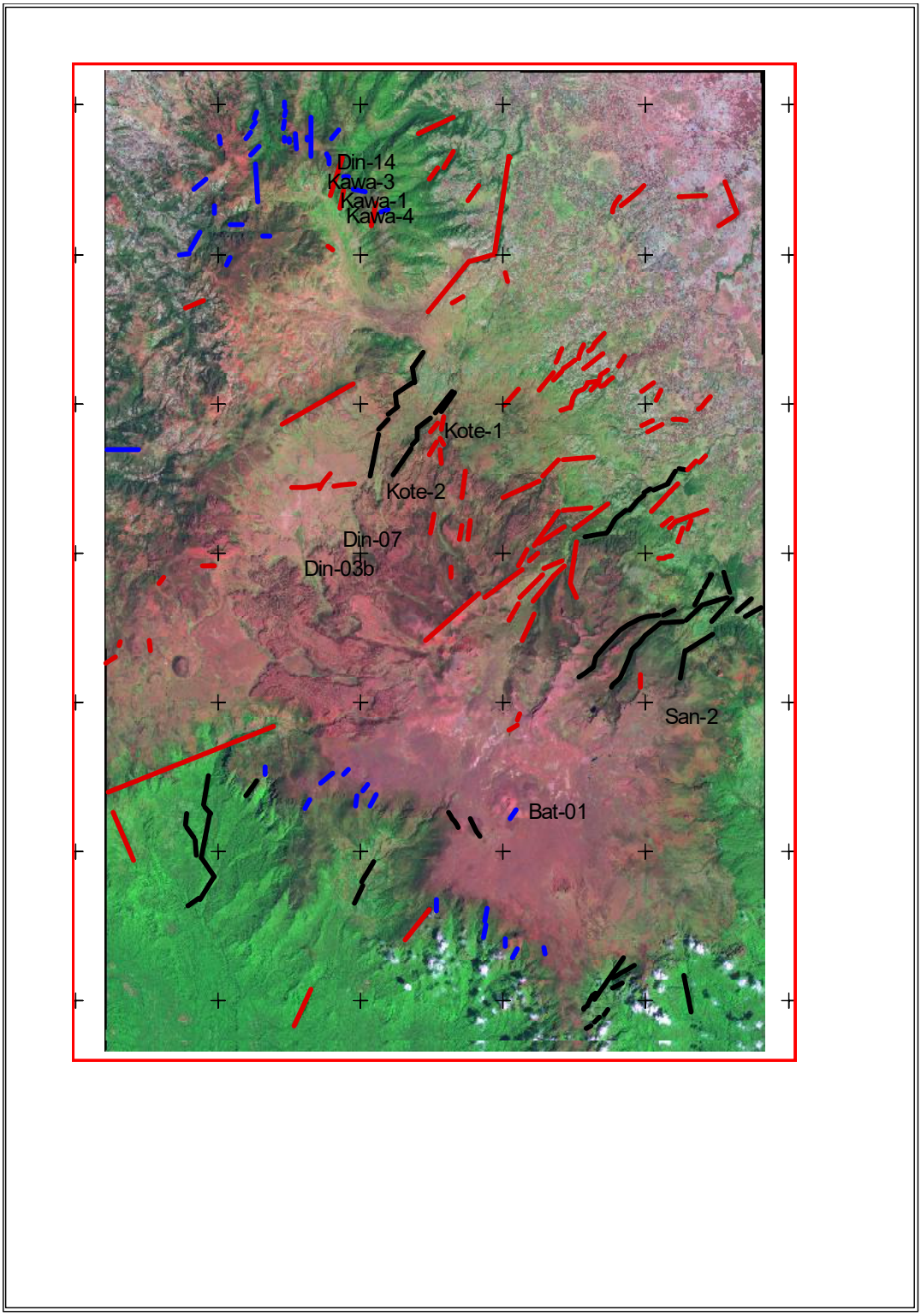

Figure 4.10 Dykes, faults, lineaments and thin section location on Bale Mountains and the surrounding areas.

5.1.1 Drainage density

The drainage density depends on the slope, nature and attitude of bedrocks and the existing regional and local fracture patterns. They reflect the lithology and structure of a given area and can be of great value for groundwater resources evaluation. Drainage density is approached in two ways with respect to groundwater: the drainage pattern and the drainage density. In the study area denderitic, trellis and parallel types of drainage patterns are recognized. Parallel types of drainage patterns are indicative of the presence of structures that act as conduits or storage for sub-surface water. These structurally controlled drainage patterns are observed NE part of the study area. The denderitic drainage pattern is the manifestation of lithological and topographic homogeneity.

The drainage density with respect to groundwater potential is determined by analysing the drainage density calculated using the stream length within grid area. Higher the drainage density the lesser the infiltration capacity that is low void ratio of the terrain which in turn the lesser the groundwater potentiality. This is because much of water coming as rainfall goes as run off. In general drainage density is the most important parameter that control groundwater occurrence and distribution.

Due to the lack of software that directly calculate drainage density, a methodology is designed by integrating different softwares. Different analyses on different softwares were applied to map the drainage density. The first step is generating the grids, which are done on AutoCAD Map 2000 engineering application software. The grids with 4km2 area having 24 columns and 32 rows is exported as *.dxf format to Arcview 3.2 to carry out the clipping of the drainage by each grids. The *.dxf format is changed to *.shp then the *.dbf file is edited to assign ID for each grids on Microsoft excel and clipping according to the ID is done by loading the geoprocessing extension. Then, the clipped drainages were imported to MapInfo professional 6.00 software to determine the length of the drainage. Database for each clipped drainage and the area of the grid 4km^2 were entered on Microsoft excel worksheet to calculate the drainage density. Finally coordinates were assigned for the centre of each of 768 grids to get point data of drainage density (Figure 5.1). The drainage density were calculated in each of the grid area using the following formula:

$DD=\sum L/A$ where, DD= Drainage density, L=Total length of streams with in 4km^2 grid, and A=Area of the grid.

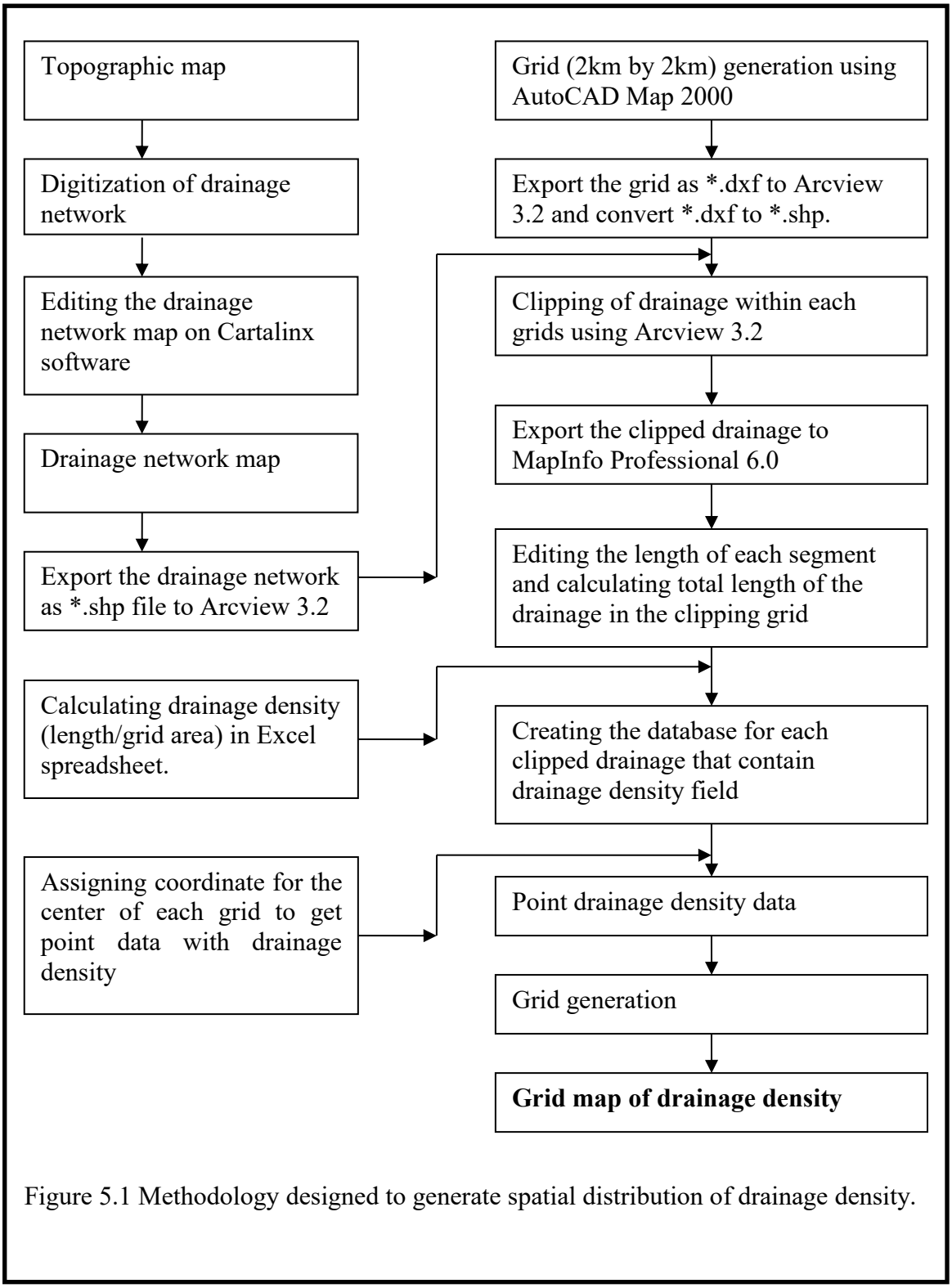

Figure 5.1 Methodology designed to generate spatial distribution of drainage density.

Using Arcview 3.2, the point drainage density data were interpolated using IDW (Inverse Distance weighted) nearest neighbor interpolation technique having output grid cell size of 100m. 768 drainage density point data is classified into four groups based on logical reasoning considering the variation of drainage density that affect groundwater occurrences of the area (Table 5.1)

Table 5.1 WEIGHTAGE OF DRAINAGE DENSITY FOR GROUNDWATER POTENTIALITY (AVAILABILITY)

	Criteria	**Classes**	**Weight**
1	Drainage density (km/km square)	0-0.9	5
		0.9-1.9	3
		1.9-2.9	2
		2.9-21	1

Figure 5.3 and figure 5.4 show the drainage network and drainage density grid map of the study area respectively.

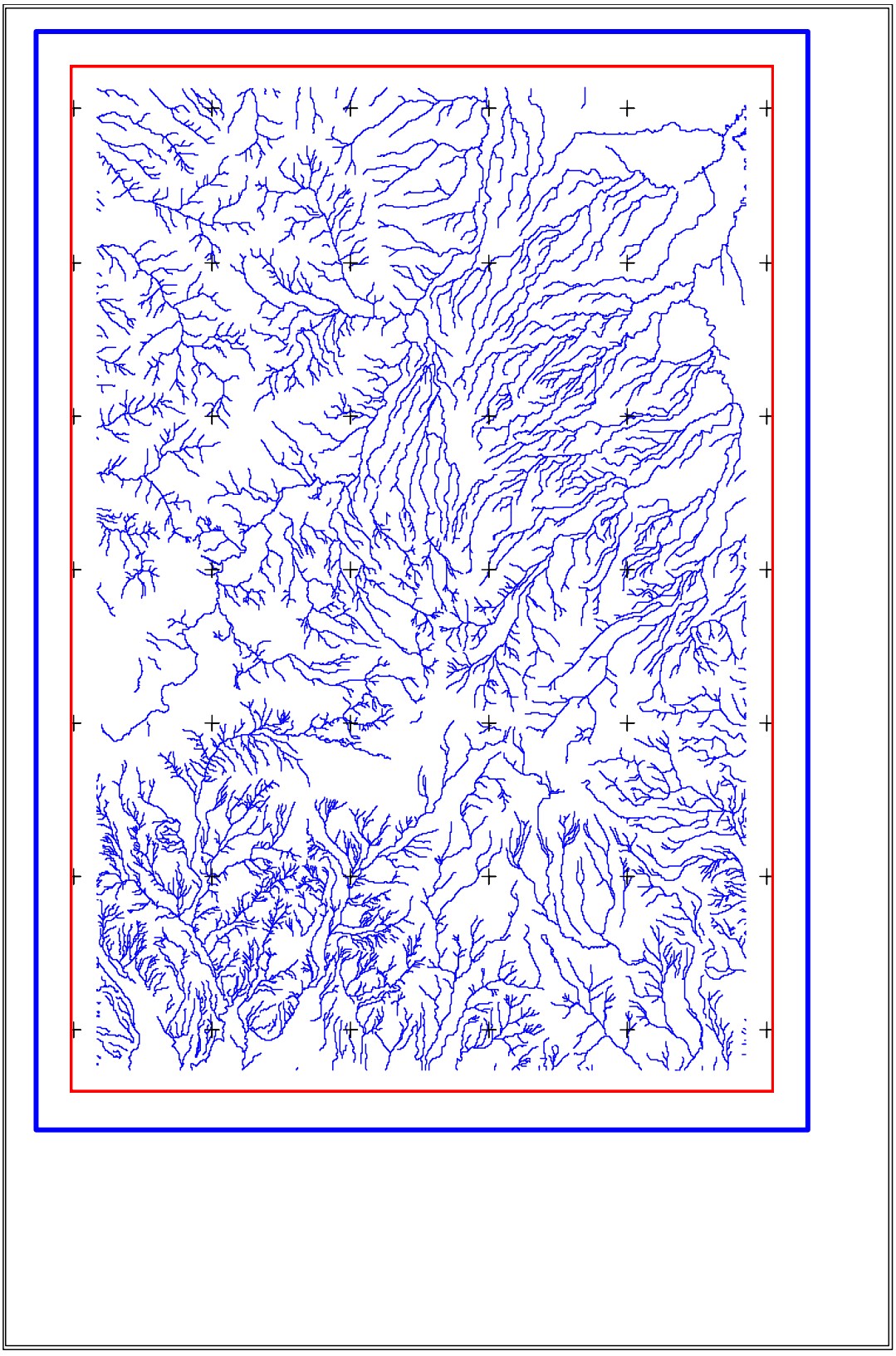

Figure 5.3 Drainage network map of the Bale Mountains and the surrounding areas

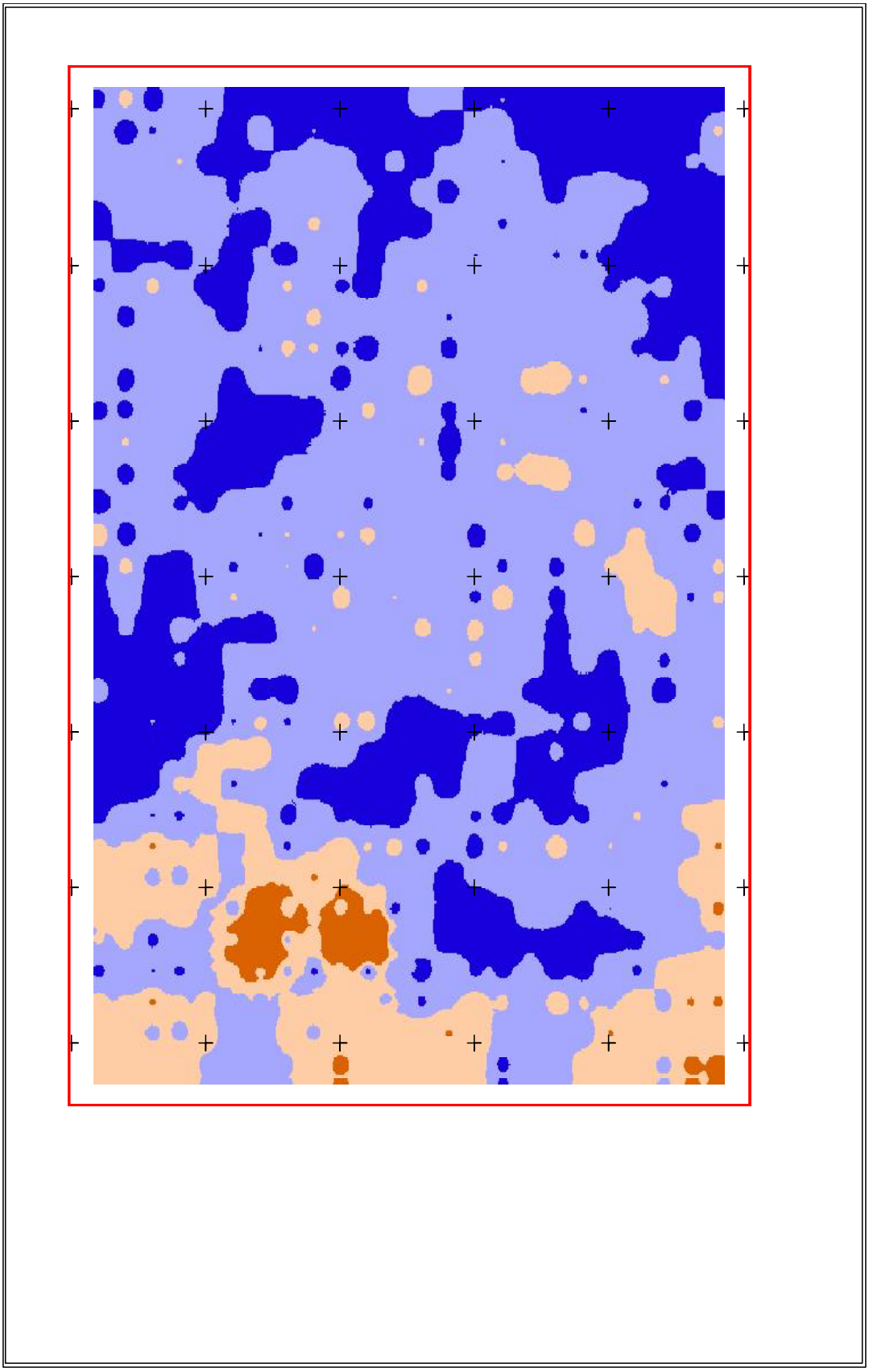

Figure 5.4 Drainage density map of the Bale Mountains and the surrounding areas.

5.1.2 Slope steepness

Slope plays an important role in influencing the recharge of groundwater depending on the degree of gradient of the landscape. The study area lies topographically at higher elevation and having flat to dissected sloppy morphology. Flat areas are capable of holding the rainfall and facilitate recharge to groundwater as compared to steep slope area where water moves as runoff quickly. Slope was generated from elevation contour digitized from 1:50000 topographic maps prepared by Ethiopian Mapping Authority. TIN were generated from 20 m interval contour and then converted to grid using IDW nearest neighbor interpolation techniques with 100 m out put grid cell size. The grids were reclassified into 5 classes based on their relevance to groundwater recharge. (Table 5.2) and (Figure 5.5)

Table 5.2 WEIGHTAGE OF SLOPE FOR GROUNDWATER POTENTIALITY (AVAILABILITY)

Layer	**Criteria**	**Classes**	**Weight**
2	Slope (in degrees)	0-6	6
		6-12	5
		12-24	3
		24-58	2
		58-75	1

The Sanetti plateau have distinct geomorphologic feature that characterizes smooth rolling plain, with small alpine lakes and swamps distributed on Sanetti plateau (Figure 6.5). The Sanetti plateau extends between 3800 and 4050m a.s.l. (Sabine and Georg Miech, 1994). One of the alpine lakes for example the Garba Gurecha Lake recharged by springs that originates from the surrounding mountains (Figure 5.6a). The northeastern and west central part is also morphologically characterizes flat areas as it is shown from slope (0°-6°). Towards southern, southeastern and southwestern, the Sanetti plateau starts to change its elevation abruptly into very rugged escarpment known as Harenna escarpment, which has slope ranges dominantly from 12°-75°. North of Sanetti plateau, Eastern, and northwestern part of the study have rugged topography.

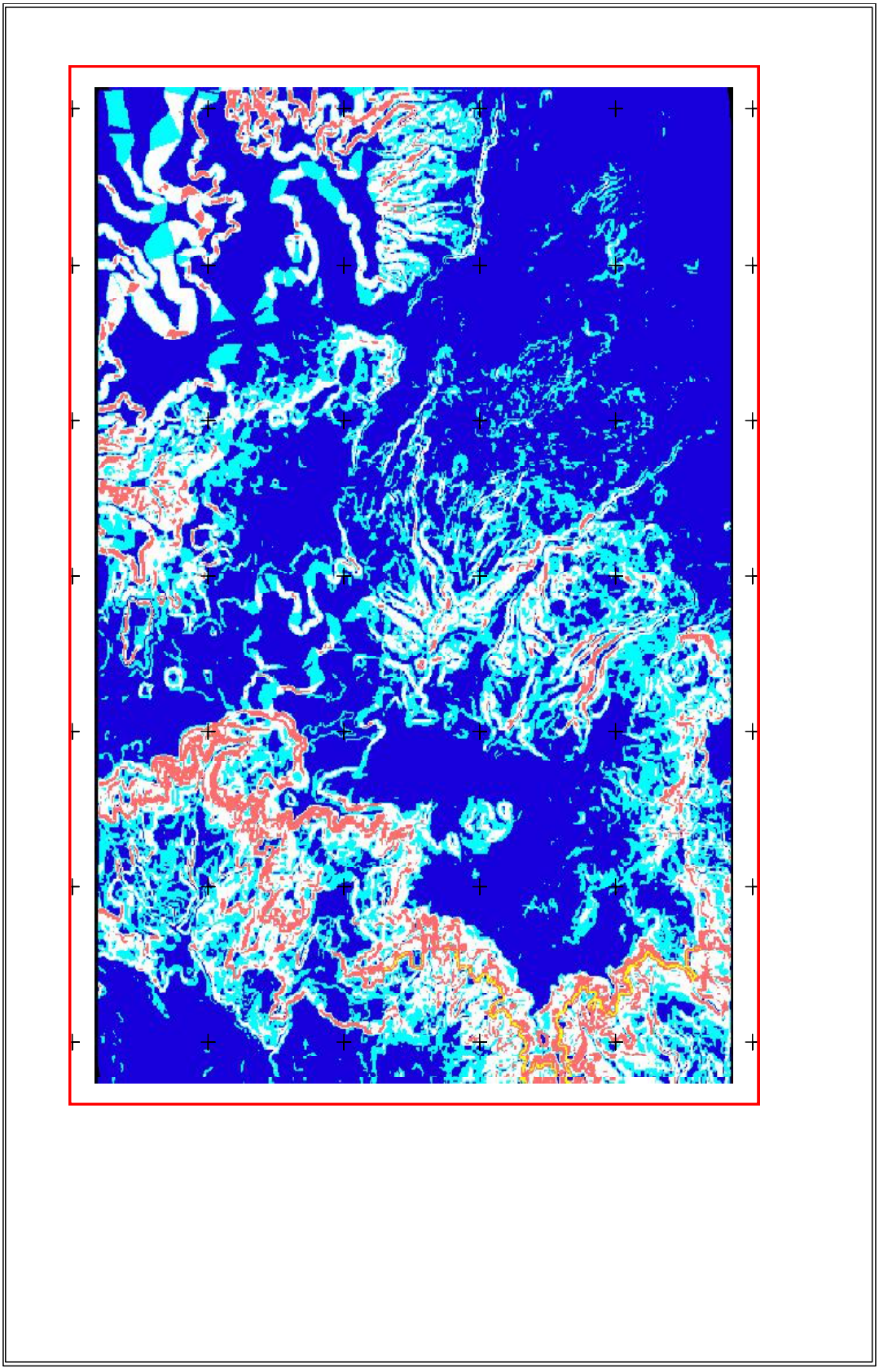

Figure 5.5 Slope map of the Bale Mountains and the surrounding areas.

Figure 5.6a One of Afro-alpine lakes, Garba Gurecha, on Sanetti plateau where recharged from springs originated from the surrounding highland.

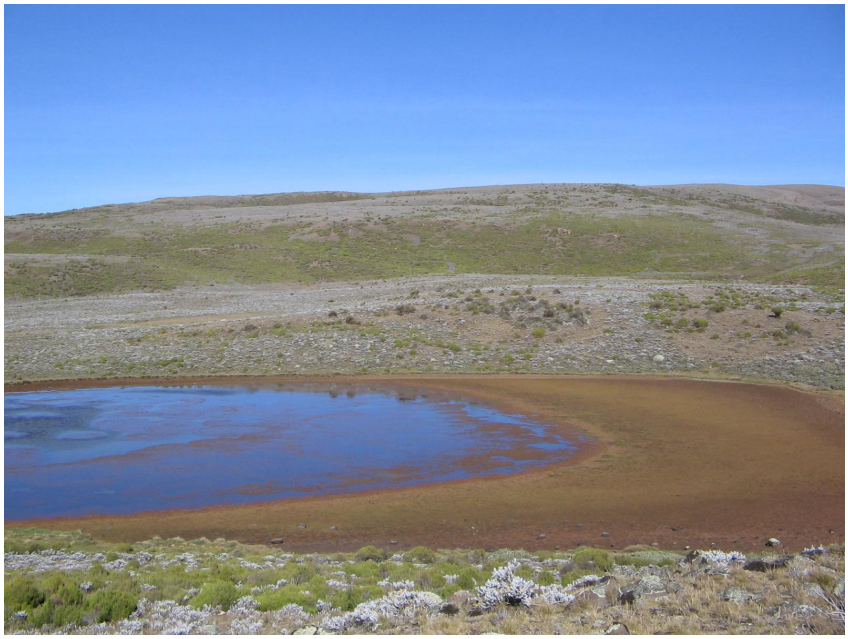

Figure 5.6b The Afroalpine Lake and the associated swamp showing the retreating of the lake.

5.1.3 Elevation

Topographic information has been collected from topographic map prepared by Ethiopian Mapping Authority at the scale of 1:50,000 scale and TIN has been generated from 20 m contour interval. The elevation in the study area ranges from 1760 m to the highest peak at Tullu Dimtu, 4377 m. Grid were generated from TIN and seven classes of elevation were made. Many springs emerges out at lowlands are originated from bale mountains. Water tends to store at lower topography than at higher topography as a reason high weight is assigned for lower elevation areas as compared to higher elevations (Table 5.3) and Figure 5.7

Table 5.3 WEIGHTAGE OF ELEVATION FOR GROUNDWATER POTENTIALITY (AVAILABILITY)

Layer	Criteria	Classes	Weight
7	Elevation (m)	1760-2134	7
		2134-2509	6
		2509-2883	5
		2883-3257	4
		3257-3631	3
		3631-4006	2
		4006-4380	1

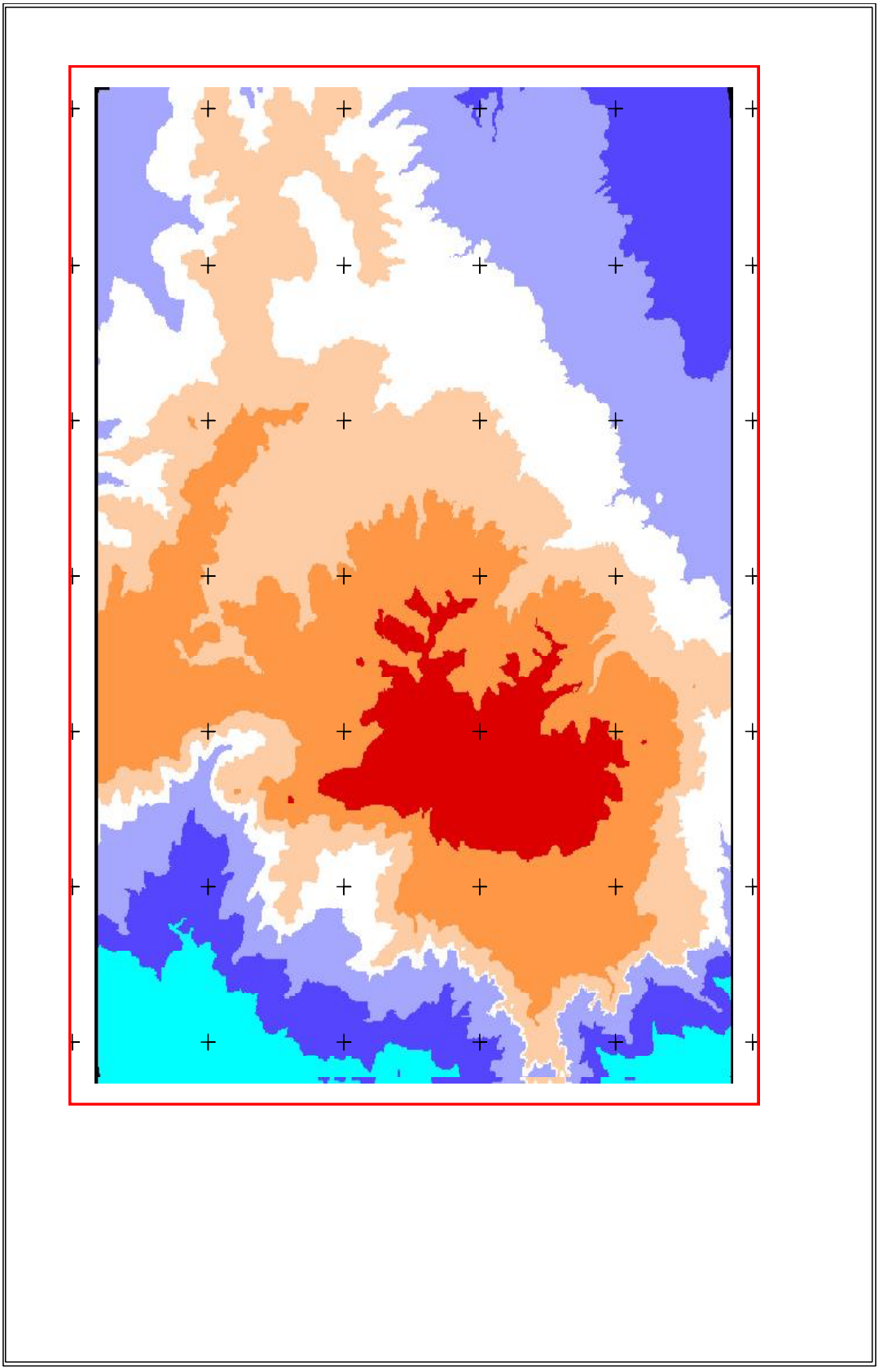

Figure 5.7 Elevation map of the Bale Mountains and the surrounding areas.

5.1.4 Landcover

One of the parameter that influence the sub surface groundwater occurrence is the present condition of landcover and landuse of the area. The effect of landcover/landuse is manifested by either by reducing runoff and facilitates recharge or trap water on their leaf and water droplets go down to recharge groundwater or negatively they facilitate loss by evapotranspiration (especially in arid and semi-arid areas). For this particular case, the effect of evapotranspiration, interception assumed to be constant. Keeping this assumption, the effect of landcover on runoff was investigated. The landcover map at the scale of 1:100000 prepared by woody biomass inventory and strategic planning and confirmed using remote sensing techniques. The general classification comprises about 5 classes after regrouping the similar classes in a way that is suitable for groundwater prospecting (Table 5.4). Figure 5.8 shows the landscape with the associated vegetation belts and figure 5.9 shows landcover map of the study area.

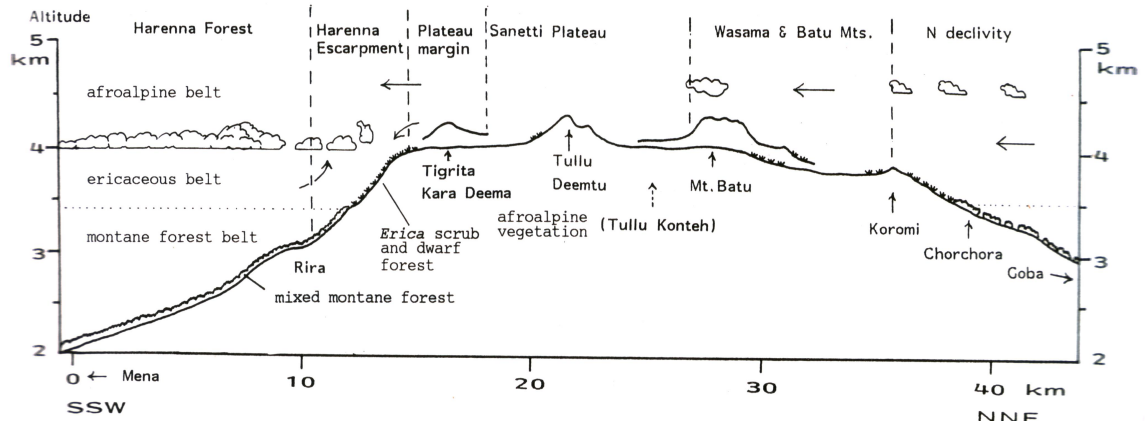

Figure 5.8 Main landscape units of the Bale Mountains; cross section runs from SW-NE. The three belts of the present vegetation are indicated (Sabine and Georg Miech, 1994)

Table 5.4 WEIGHTAGE OF DIFFERENT LANDCOVER FOR GROUNDWATER POTENTIAL (AVAILABILITY)

Layer	Criteria	Classes	Weight
4	Landcover	Natural forest	5
		Afro-alpine; Erica /Hypericum	4
		Cultivated land	3
		Afro-alpine; Grassland/Mooreland	2
		Grassland/unstocked(woody plant)	2

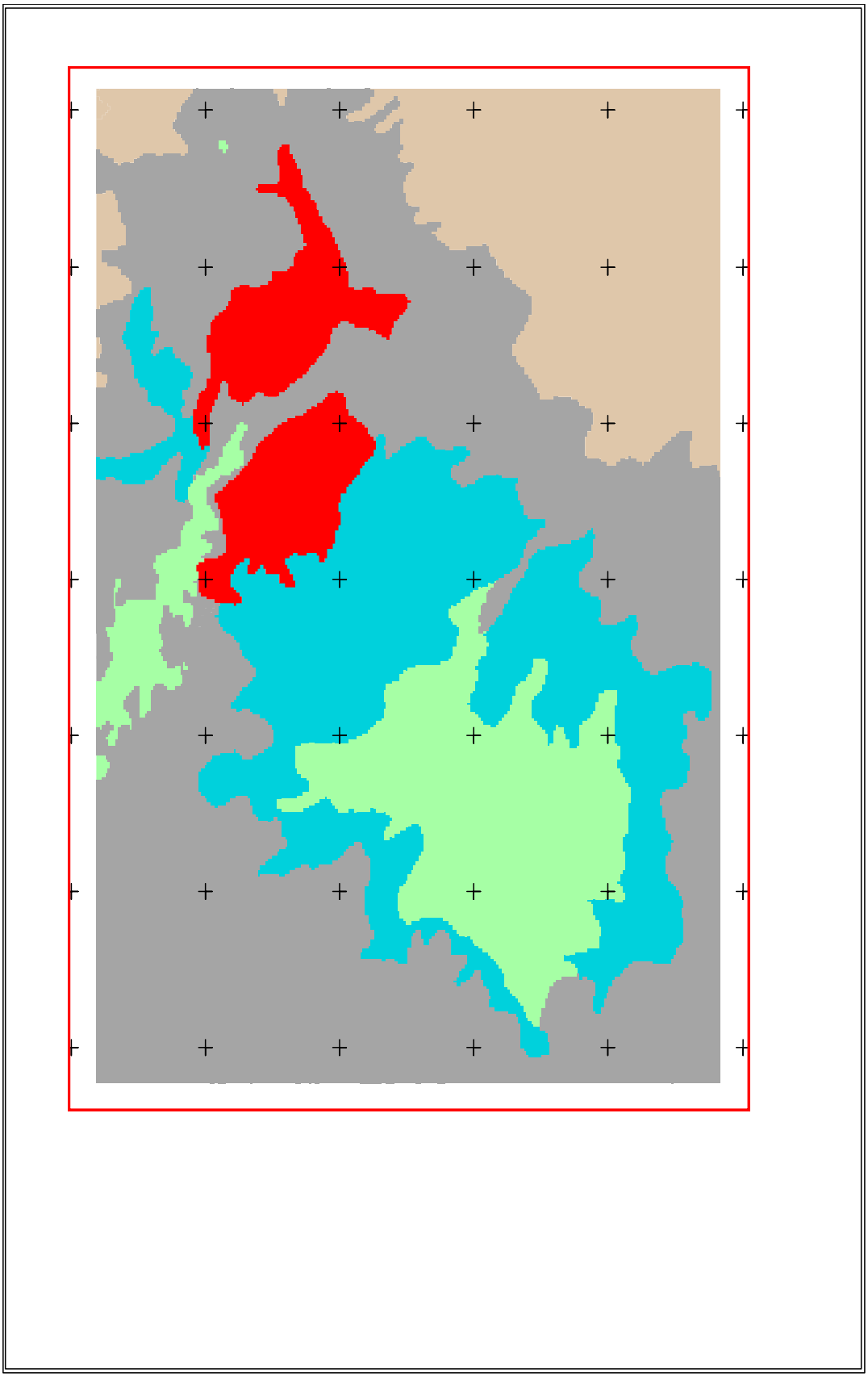

Figure 5.9 Landcover map of Bale Mountains and the surrounding areas.

The Harenna forest is one of thick extensive the natural forest in Ethiopia. It has significant contribution in controlling the runoff coming from the plateau as a result first priority has been given. The second weight is given to the Ericaceous belt, which contains 8 m tall Erica dominated trees to 1-3 m tall scrub. The scrub is more or less open and being composed of different regeneration stages (Sabine and Georg Miech, 1994). The Erica scrub gradually disintegrate into 1.5 m to 0.5 m low solitary shrubs of spherical shapes which grow more or less closed these are the Afroalpine; grassland/moreland and third priority has been given (Figure 6.10). The cultivated land characterized by intensive cultivation and permanently coverd by crops. The last priority has been given to the grassland/unstocked (woody plant) is characterized by expansion of settlement and the land is becoming degraded as a consequence runoff is increasing.

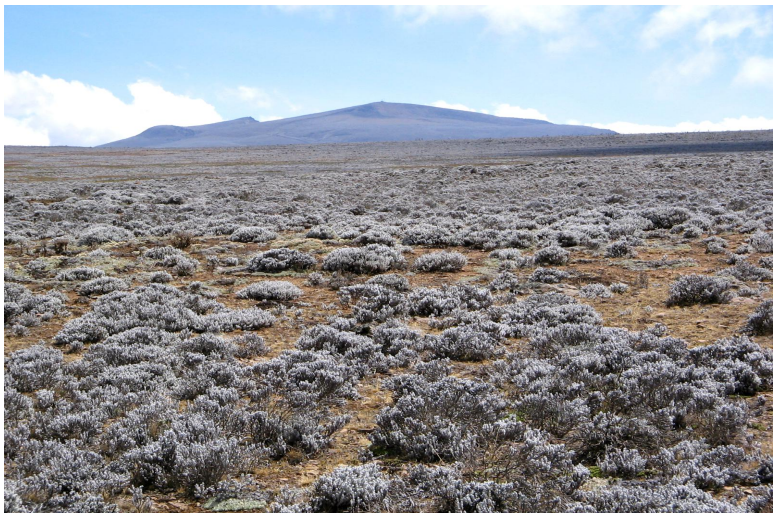

Figure 5.10 The Afroalpine vegetation on Sanatti plateau.

5.1.5 Soil

The soil forming factors, climate, parent rock, vegetation, fauna and physiography are responsible for the type of soil formed and plays an important role on groundwater recharge through infiltration and loss through run-off. The type of soil and permeability affects the water holding and infiltrating capacity of a given soil. The Bale Mountains are entirely covered by volcanic products, the soils, mainly derived from basaltic and trachytic parent rock, are fairly fertile silty loams of reddish-brown to black color (Sabine and Georg Miech, 1994). Table 5.5 and Figure 5.11

The soil classes used for the groundwater investigation are based on the hydrologic property of FAO classification of soil FAO, (2001). In the study area there are about 6

types of soil classes. These are Cambisols, Histosols, Nitosols, Luvisols, Lithosols, and Vertisols (Table 6.5)

Cambisols

Most Cambisols are medium-textured and have a good structural stability, a high porosity, and good water holding capacity and good internal drainage. Most Cambisols also contain at least some weatherable minerals in the silt and sand fractions. Based on these characteristics, Cambisols have good infiltration capacity to recharge groundwater.

Histosols

Soil formed in organic containing material, incompletely decomposed plant remains, with or without admixtures of sand, silt or clay. It has large total pore volume of Histosols (typically > 85). Fibric Histosols are loosely packed in their natural state. Histosols are unlike all other soils in that they are formed in organic soil material with physical, chemical and mechanical properties that differ strongly from those of mineral soil materials. Organic soil material is soil material that contains more than 20 percent organic matter by weight, roughly equivalent to 30 - 35 percent by volume. Histosols that formed in organic soil material under the permanent influence of groundwater.

Nitosols

Nitosols are deep, well-drained, red soils. Finely textured weathering products of intermediate to basic parent rock, possibly rejuvenated by recent admixtures of volcanic ash. The clay assemblage of Nitisols is dominated by kaolinite. Nitisols are rich in iron and have little water-dispersible clay. It is red or reddish brown clayey soils. They are well-drained soils with a clayey subsurface horizon. Nitisols are free-draining soils and permeable to water (50-60 percent pores). Their retention of `plant-available' moisture is only fair (5-15 percent by volume) but their total moisture storage is nonetheless satisfactory because the rootable soil layer extends to great depth, commonly deeper than 2 m. Most Nitisols can be tilled within 24 hours after wetting without serious deterioration of the soil structure.

Luvisols

Luvisols have distinct clay accumulation horizon. Most Luvisols are well drained but Luvisols in depression areas with shallow groundwater may develop gleyic soil properties in and below the argic horizon. Stagnic properties are found where a dense illuviation horizon obstructs downward percolation and the surface soil becomes saturated with water for extended periods of time. Soils in which clay is washed down from the surface soil to an accumulation horizon at some depth.

Leptosols

Leptosols accommodates very shallow soils over hard rock, within 25 cm from the soil surface, mostly land at high or medium altitude and with strongly dissected topography. Leptosols are found in all climatic zones, particularly in strongly eroding areas. Leptosols are genetically young soils and evidence of soil formation is normally limited to a thin A-horizon over an incipient B-horizon or directly over the unaltered parent material. Stagnic properties can occur in Leptosols on gentle slopes or in pockets but are rather exceptional. Their shallowness and/or stoniness, and implicit low water holding capacity. Swelling and shrinking smectitic clays in the mineral residue are accountable for the dominance of blocky structures. The excessive internal drainage of many Leptosols can cause drought even in a humid environment.

Vertisols

Commonly known as black cotton soil containing smectite clay that characterize sticky nature and have high water holding capacity and low infiltration capacity. Vertisols become very hard in the dry season and are sticky in the wet season. Tillage is difficult, except for a short period at the transition between the wet and dry seasons.

Table 5.5 WEIGHTAGE OF SOIL FOR GROUNDWATER POTENTIAL (AVAILABILITY)

Layer	Criteria	Classes	Weight
3	Soil	Cambisols	5
		Histosols	4
		Nitosols	3
		Luvisols	2
		Leptosols	1
		Vertisols	1

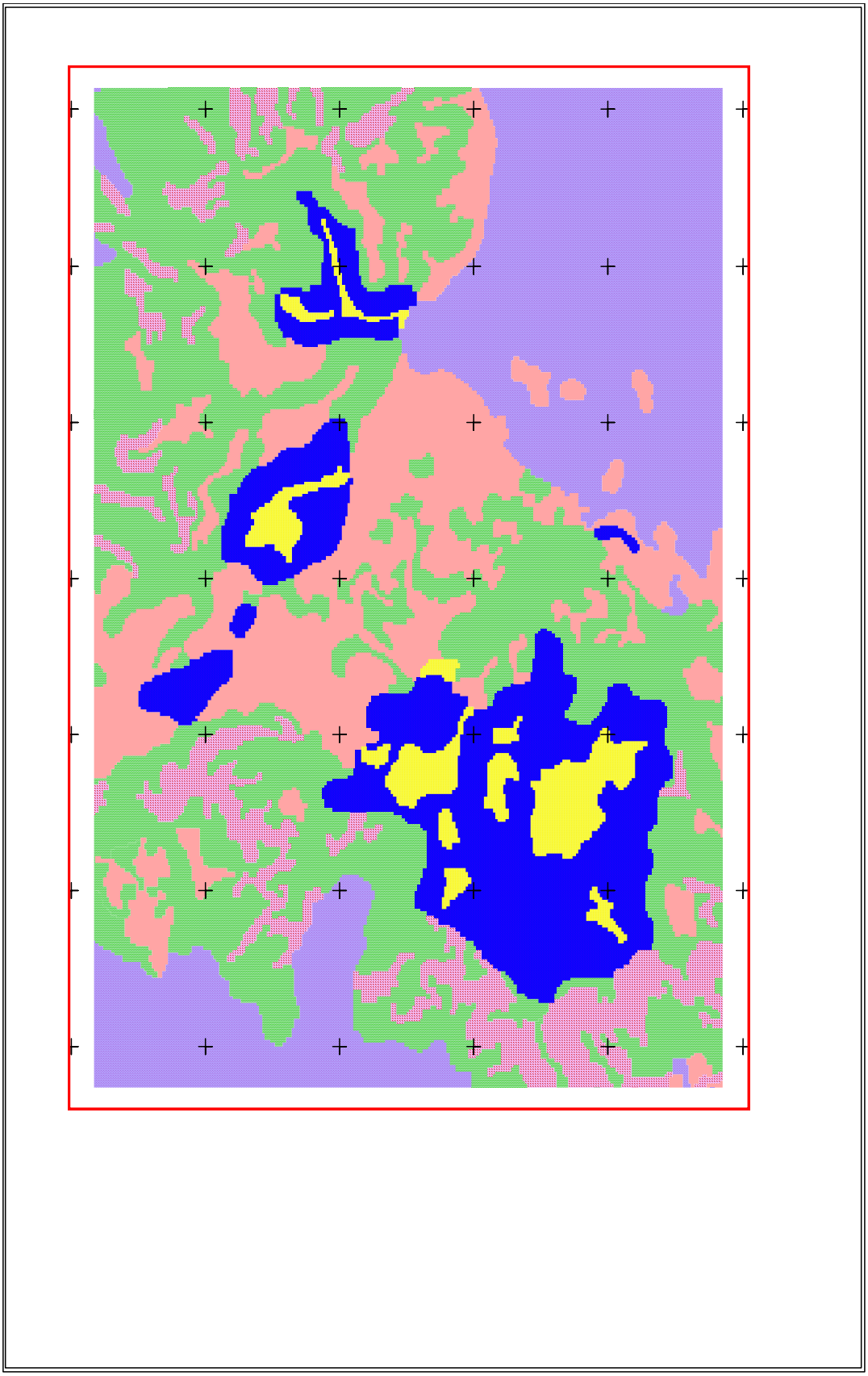

Figure 5.11 Soil map of Bale Mountains and the surrounding areas.

5.1.6 Rainfall

Rainfall is one of the major sources for groundwater. The high rainfall amounts imply the possibility of high groundwater recharge and vice versa. The area characterized by high rainfall amount shows high groundwater potential zones. Spatial distribution of rainfall was generated using rainfall data from National Meteorological Services Agency. Due to uneven distribution of the rainfall stations the rainfall data might not indicative of the exact figure but it gives workable rainfall distribution. In addition to 7 rainfall stations data of the past 10 years taken from National Meteorological Services Agency, 3 stations records of mean annual rainfall from the year 1985-1991 were added from a book entitled with Ericaceous Forests and Heathlands in the Bale Mountains of South Ethiopia; Ecology and Man's Impact to increase meaningful distribution of rainfall. The isohyetal map were generated from point rainfall with out put grid cell size of 100 m using IDW nearest neighbor interpolation techniques. Then rainfall is classified into 4 regions and weight is assigned based on their relevance to groundwater exploration (Table 5.6)

Table 5.6 WEIGHTAGE OF SLOPE OF FOR GROUNDWATER POTENTIAL (AVAILABILITY)

Layer	Criteria	Classes	Weight
5	Rainfall (mm)	1042-1105	5
		979-1042	4
		915-979	3
		852-915	2

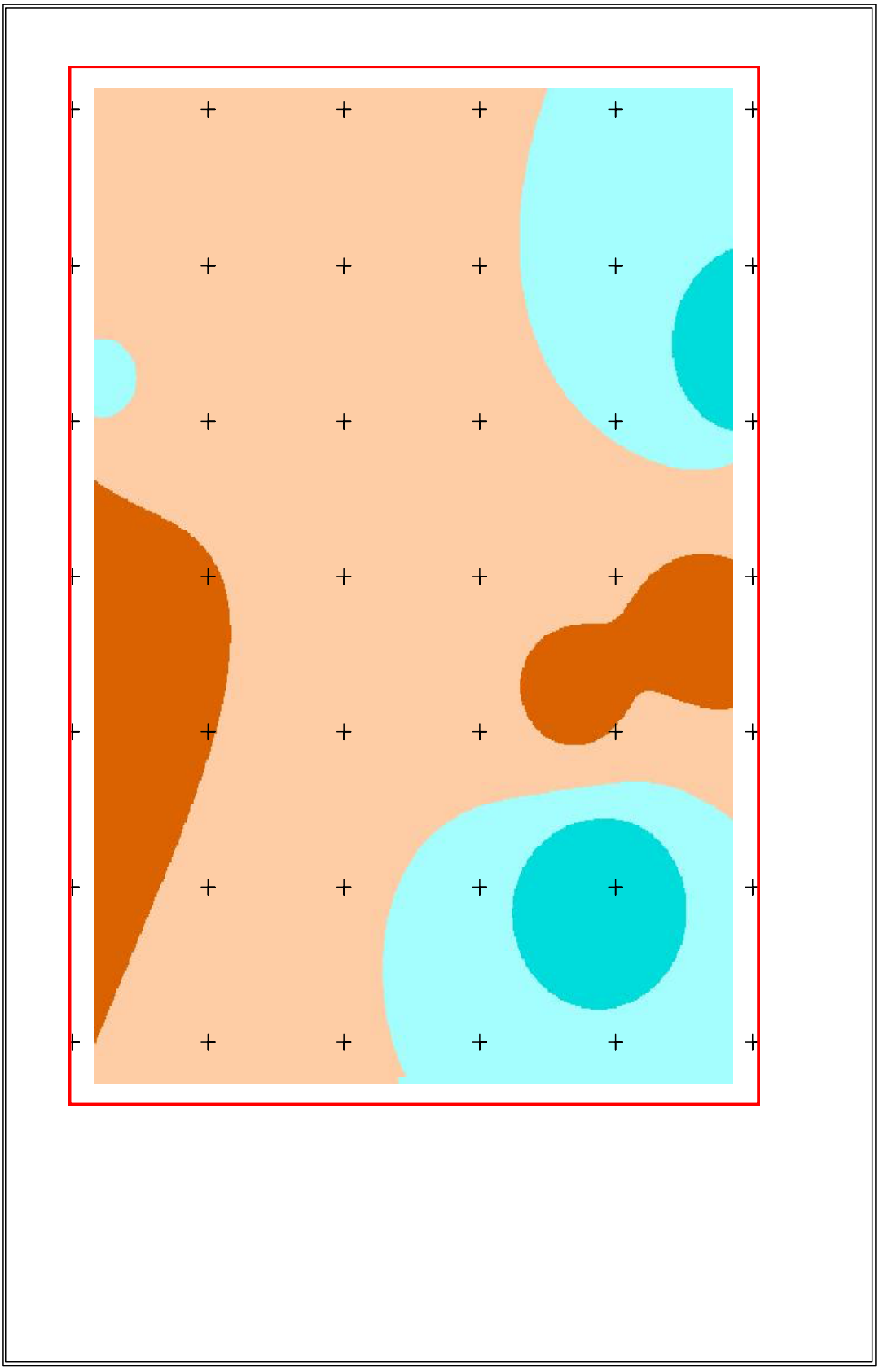

Figure 5.12 Rainfall map of Bale Mountains and the surrounding areas.

5.1.7 Lineaments

Faults and dykes are discontinuous earth's features that can be more easily identified and extrapolated on image than on the ground. These features are mapped as lineaments (indicators of subsurface fractures) influencing the occurrence of groundwater acting as conduits and/or reservoirs. The dykes can be either a conductor or a barrier depending on the intensity of fracturing. The length of dykes is also an important parameter in controlling regional subsurface water flow rather than local movement. The majority of the dykes have small thickness and length that shows their influence is on local groundwater movement rather than regional. Springs have been observed at the contact between the country rock and fractured basaltic dykes. The structures, locations, and orientations with respect to groundwater flow are very important. Mapping of the lineaments were done using false colour composite image of 742 (RGB) and each bands were investigating and compared interms of contrast and band 4 were selected because it shows good contrast and geological lineaments. Shaded relief of the also supports the lineament mapping. Distance analyses were carried out on the digitised structures (dykes, faults and lineaments) with output grid cell size of 100 m and weight has assigned based on distance to the structures. Areas close to the structures have got high weight and vice versa. Table 5.7. See (Figure 5.13 and 5.14)

Table 5.7 WEIGHTAGE OF DISTANCE TO STRUCTURES FOR GROUNDWATER POTENTIALITY (AVAILABILITY)

Layer	Criteria	Classes	Weight
7	Distance to structures (m)	0-250	4
		250-500	3
		500-12000	1

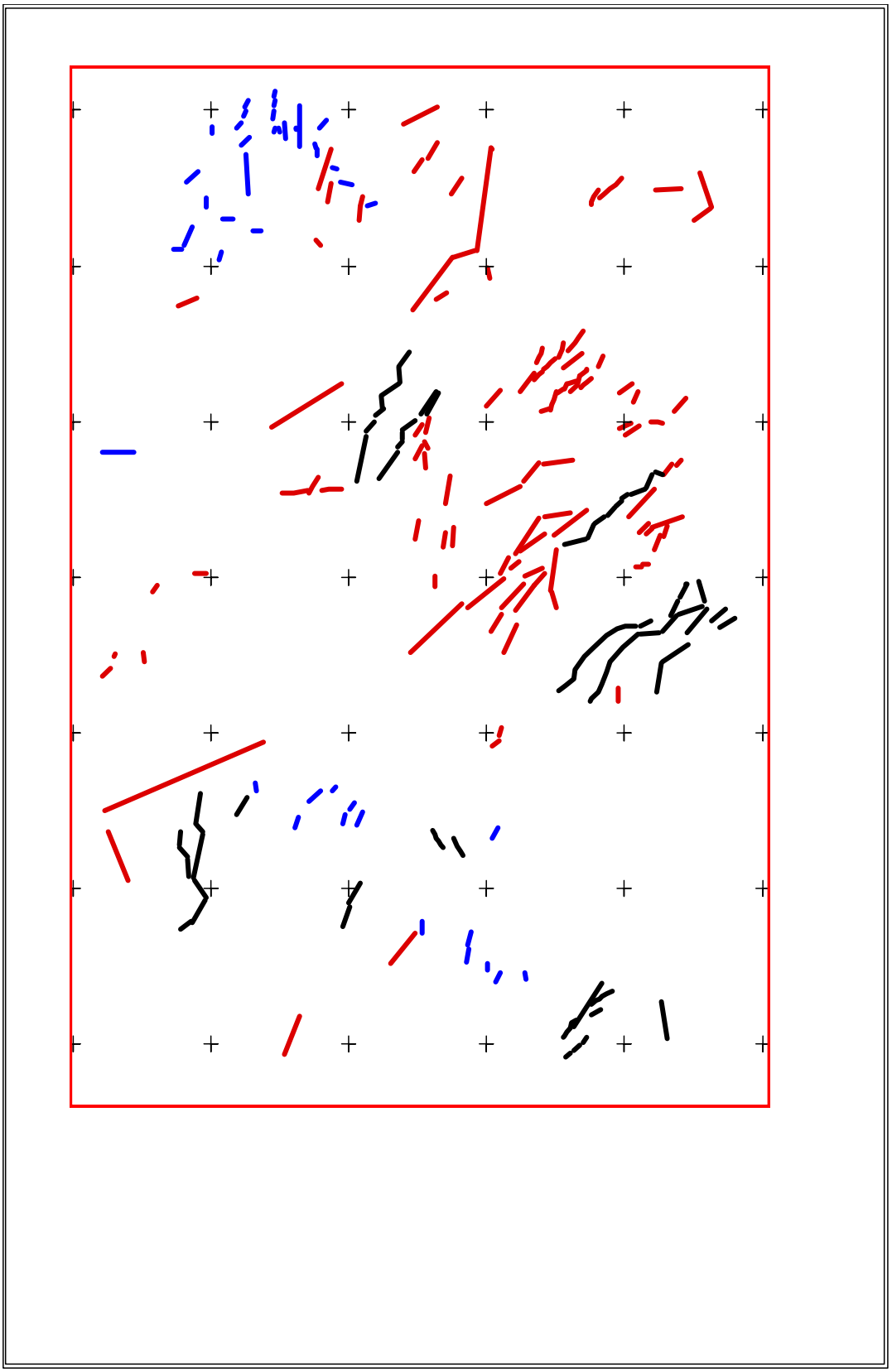

Figure 5.13 Geological structures on the Bale Mountains and the surrounding areas.

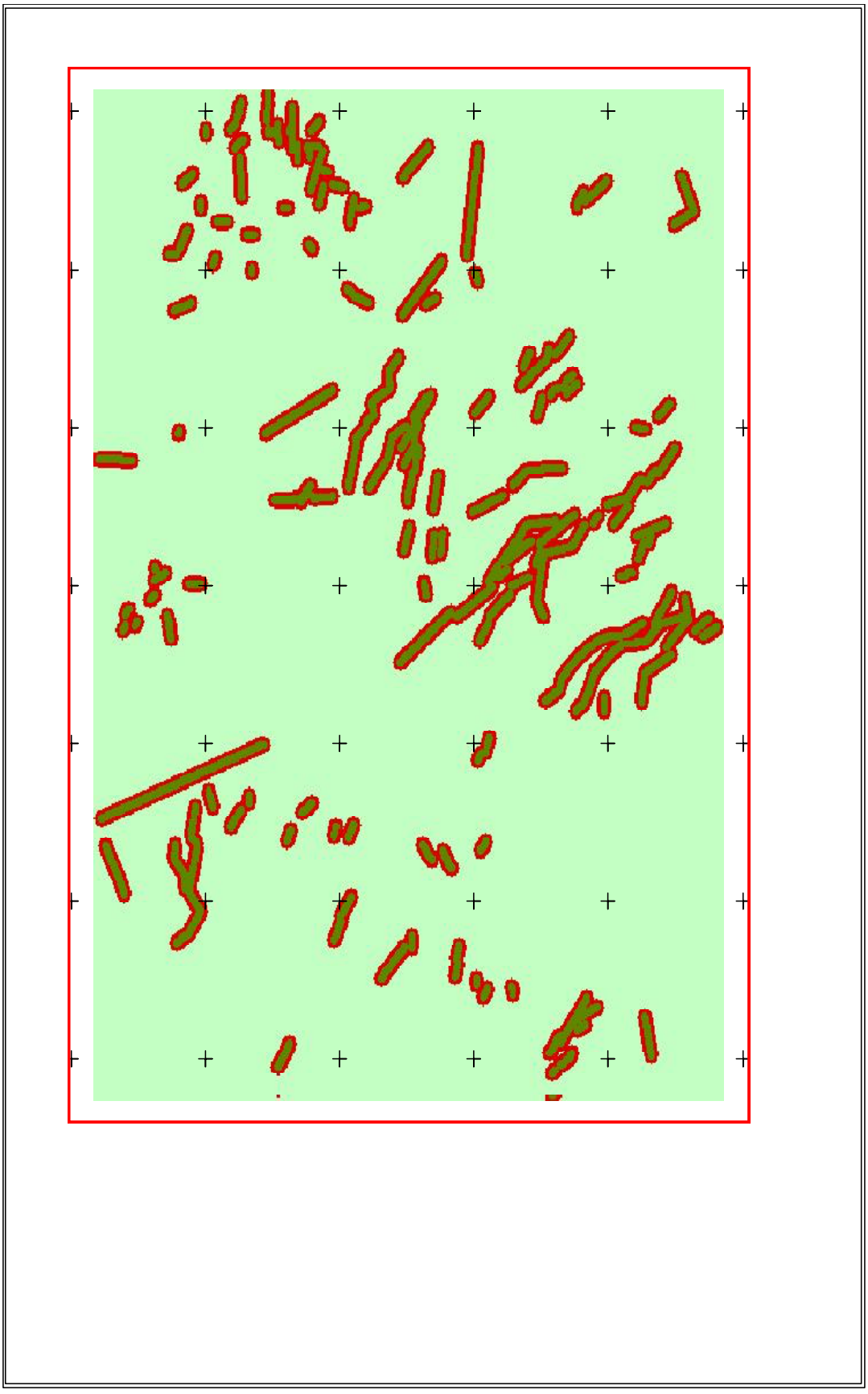

Figure 5.14 Distance to geological structures (dykes, faults and lineaments) of the Bale Mountains and the surrounding areas.

5.1.8 Biological factor (burrowing of rodents)

The extensive burrowing activities of numerous rodents especially the endemic Giant molerat, on the Bale Mountains on the level ground of broad valleys Weiyb and on Sanetti plateau in the vicinity of swamps or seasonally waterlogged areas (Sabine and Georg Miech, 1994). Geysey valley is also good area for rodents. The burrowing activities give the area the appearance of ploughed field. The estimated density of Molerate ranges from between 2600 (Beyene 1986) and 6300 per square kilometre in suitable habitat (Yalden 1975). The soil is very loose, burrowed as a consequence the recharge capability of the soil is significantly enhanced. It is also seen that this action maintains the vegetations at permanent stages. The burrow system of molerat is very extensive because the species harvests only those herbs which grow within the radius of its body length from a hole, allowing it to retreat very quickly if a predator approaches (Beyene, 1986, Yalden 1975). Thus, several holes have to be opened per day to satisfy the food demand of one individual. Consequently, large amounts of soil are turned over within short time (Figure 5.15 and 5.16). The soil excavated from the burrow system and deposited around the holes is successively colonized by afroalpine pioneer herbs and grasses. The burrowing activities have been classified into three classes. (Table 5.8)

Figure 5.15 shows the burrowed soil with the rodent (Giant Molerat).

Figure 5.16 Soil affected by burrowing of rodents

Table 5.8 WEIGHTAGE OF BURROWING ACTIVITIES FOR GROUNDWATER POTENTIALITY (AVAILABILITY)			
Layer	**Criteria**	**Classes**	**Weight**
8	Biological factor (burrowing of rodents)	Intensive Burrowing activity	5
		Moderate burrowing activity	3
		Minimal burrowing activity	1

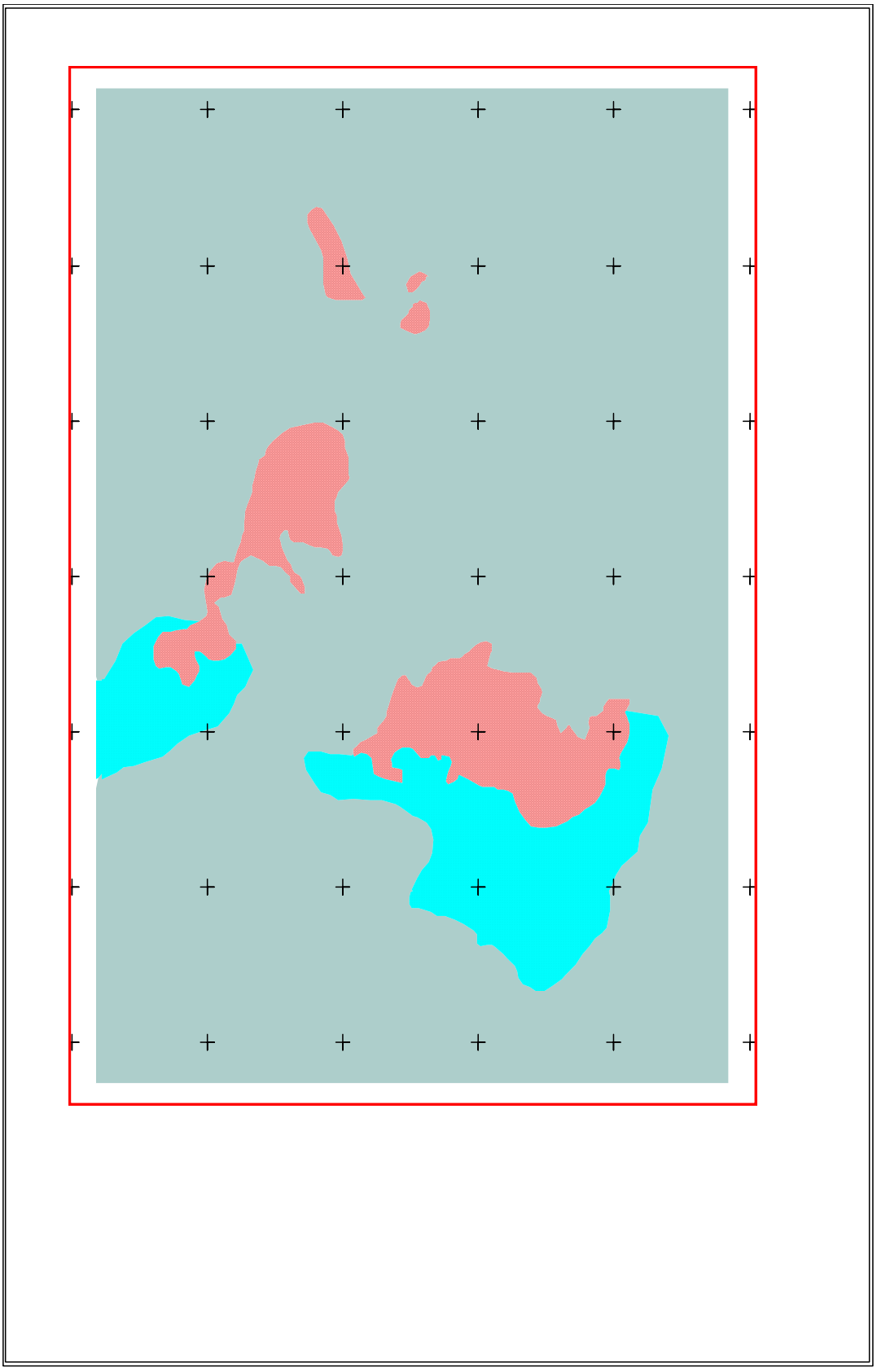

Figure 5.17 Burrowing affected areas on Bale Mountains and the surrounding areas.

5.2. Integration of thematic layers and modelling through GIS

The thematic layers include Drainage density, Slope, Elevation, Landcover, Rainfall, Soil, Geologic structures (dykes, faults and lineaments), and Biological factor (burrowing of rodents) (Figure 5.18). All point, contour and polygon data were converted to grid. Each of the class in the thematic layers was qualitatively described and reclassified by assigning numbers starting from 1 up to 7. Numbers were assigned based on groundwater potentiality of each class in layers. The higher the number the better groundwater potentiality (availability). After assigning weight the integration of all layers were carried out applying raster overlay analysis in a GIS environment (Arcview 3.2) using the following formula:

GWP=DD+EL+SL+SO+LC+RF+ST+BF Where, **GWP**=Groundwater Potential

DD=Drainage density, **EL**=Elevation, **SL**=Slope, **SO**=Soil, **LC**=Landcover, **RF**=Rainfall, **ST**=structures and **BF**=Biological factor (burrowing of rodents)

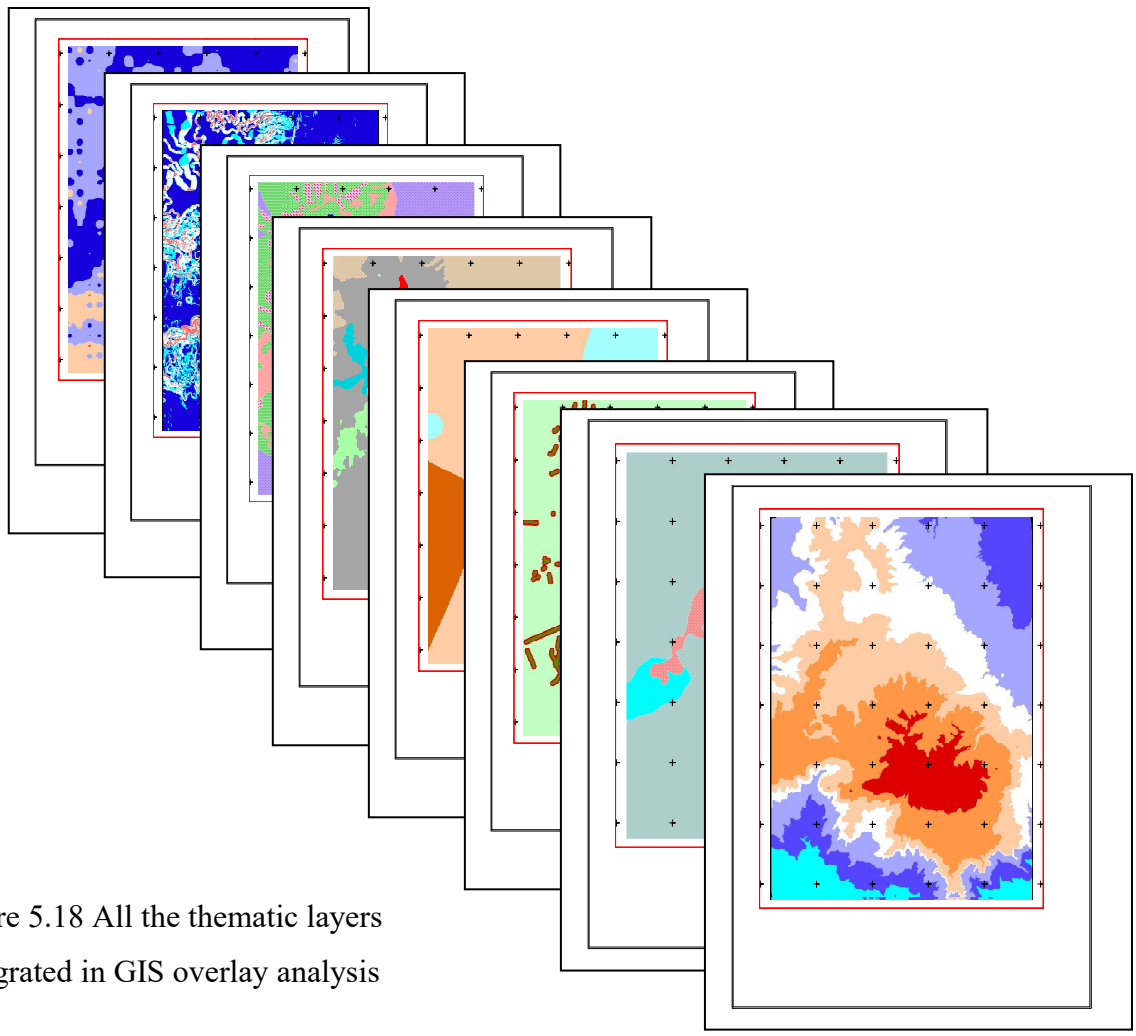

Figure 5.18 All the thematic layers integrated in GIS overlay analysis

Through this analysis the total weights of the final integrated grids were derived as the sum of the weights assigned to the classes of the different layers. The delineation of the groundwater potential zone was made by grouping the grids of the final integrated layers into different potential zones. The grouping was made by considering logical reasoning instead of dividing the maximum and the minimum value into different categories. Based on this 5 classes of groundwater potential zones were identified (Table 5.9).

Table 5.9 INTEGRATED GROUNDWATER CATEGORIES FOR GROUNDWATER PROSPECTS WITH LOWER AND WEIGHT VALUES

	Groundwater Category	Lower and upper weight values	Count of cells	Area (sq.km)
1	Very Good	37-29	31238	312.38
2	Good	28-27	39053	390.53
3	Moderate to Good	26-25	86859	868.59
4	Moderate	24-22	108120	1081.20
5	Poor	21-15	30964	309.64

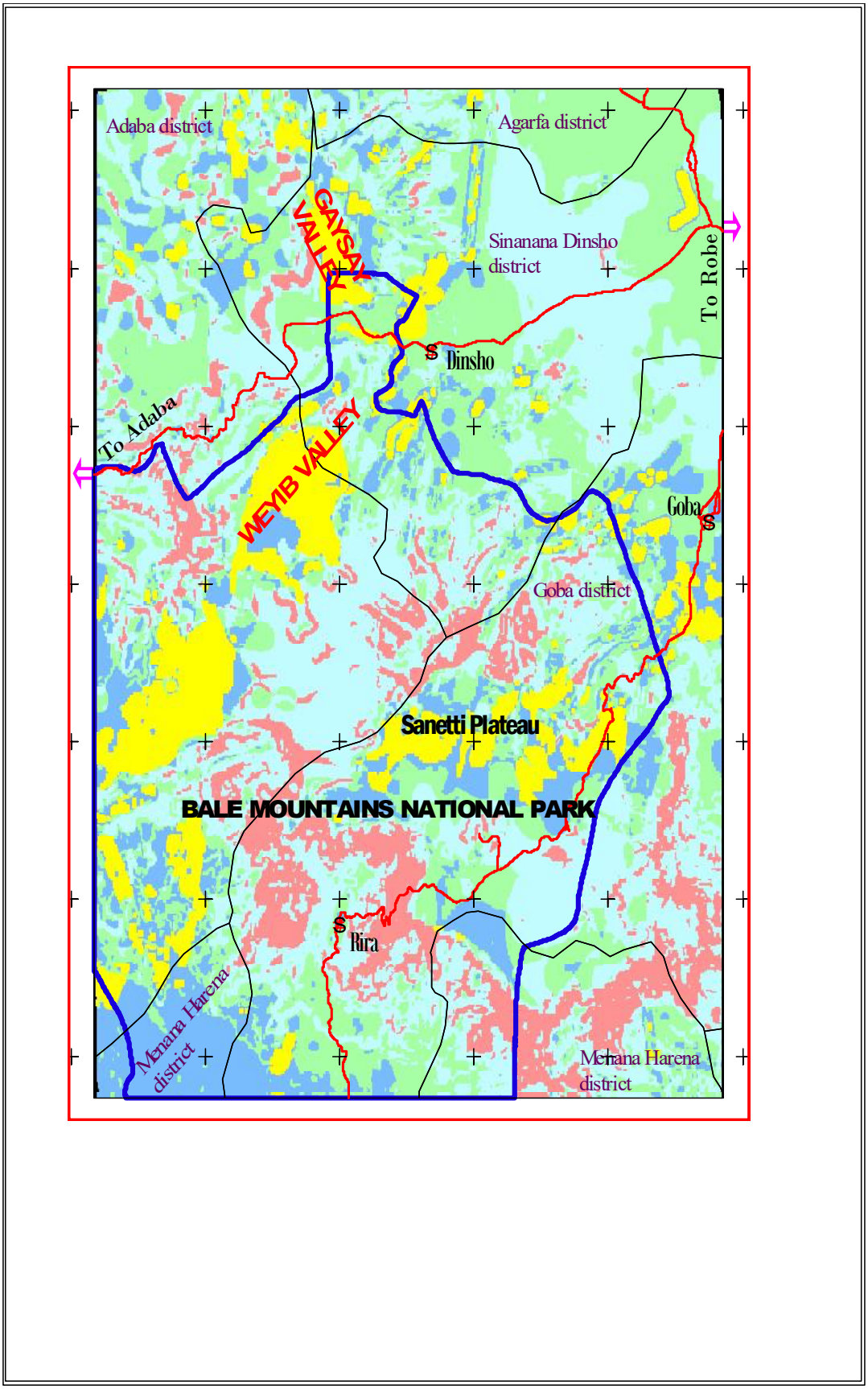

Figure 5.19 Groundwater potential zones of Bale Mountains and the surrounding areas.

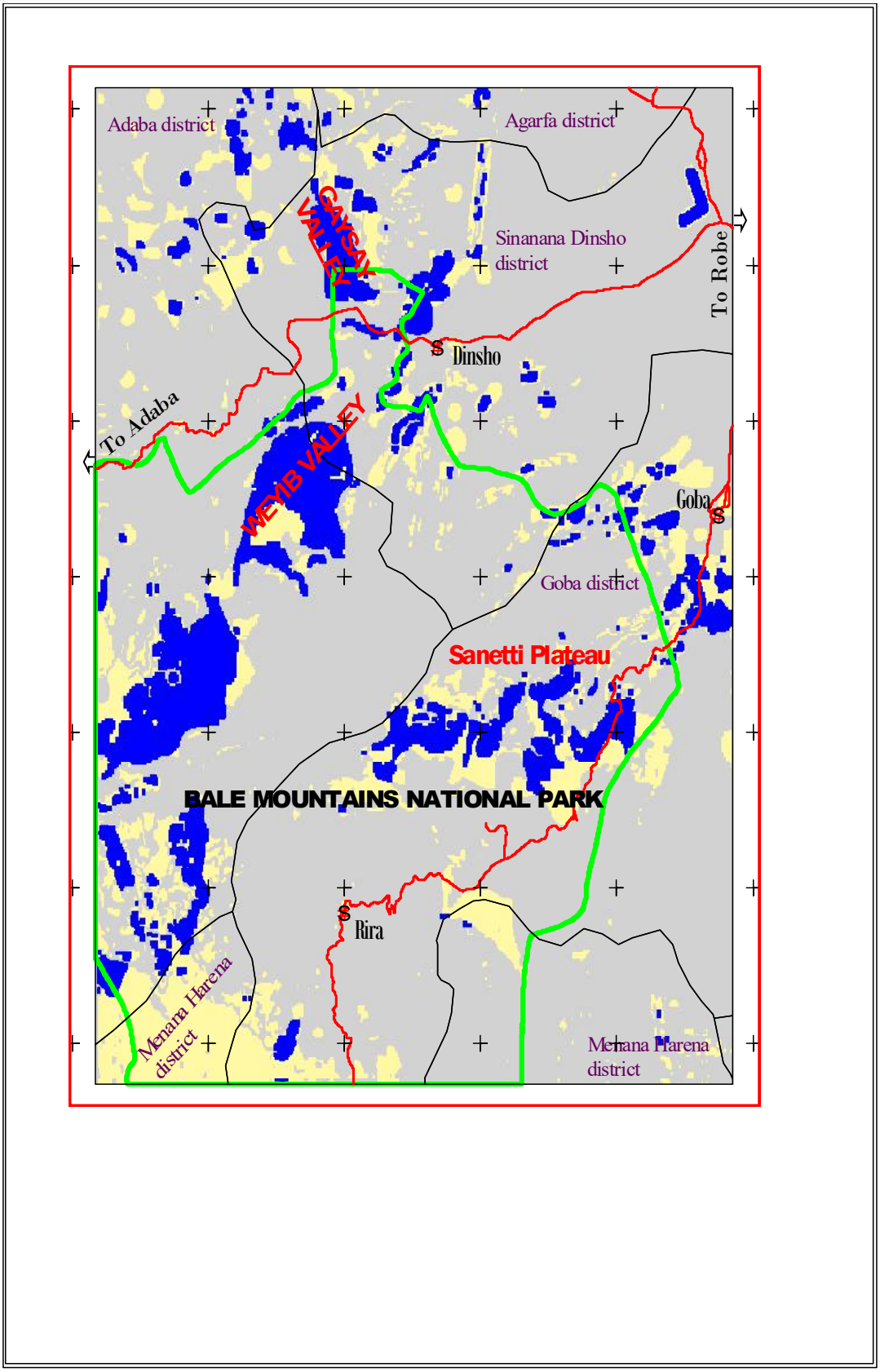

Figure 5.20 The most suitable groundwater potential zones of Bale Mountains and the surrounding areas.

5.3 Concluding remarks

The delineation of preliminary groundwater potential zones through the integration of different thematic layers obtained from remote sensing interpretation and other secondary data has found to be effective techniques for analysing the information content of each layer in GIS environment. The analysis would give meaningful results without the need of conducting fieldwork, geophysical and test drilling which are time, effort and cost consuming activities. This technique would give broad ideas about the groundwater potentiality of the areas and then minimize the areas where detail groundwater exploration activities to be carried out to study sub surface aquifer condition (storability and conductivity) through geophysics and drilling test. The outcome of the application of remote sensing and GIS on Bale mountains showed reasonable results where high potentiality on the areas of Weyib valley and Geysey valley due to the cumulative effect of high contribution of the rodents, soil, slope, drainage density, rainfall give one of the potential area for natural recharging of the aquifer of the area. The Weyib valley is one of the most important catchments of the Bale Mountain. The burrows of the Giant Molerat are confined to open, afroalpine habitat where there is high groundwater table or periodic water stagnation. The eroded and steep part of the Harenna escarpment and the rugged geomorphology on the northern part of Sanetti plateau shows less groundwater potentiality. Groundwater potential map generated through this process will help planners and decision makers for devising and feasible groundwater development plans. This type of analysis similarly can be applied at a regional scale on another part of Ethiopia where there is a significant need of water for irrigation, drinking purpose.

Table 3.3 petrographic descriptions of volcanic rocks of Bale Mountains and the surrounding areas.

Sample	Location	Rock types	Description
Din-14	576889E 797980N	Porphyritic Olivine Basalt	The rock shows porphyritic texture. The phenocrysts occupy (30 vol.%) in groundmass of (70 vol. %). The phenocrysts contain subhedral plagioclase (15 vol. %), subhedral pyroxene (10 vol. %), and euhedral olivine (5 vol. %). The (70 vol. %) groundmass is composed of lath-shaped plagioclase, anhedral pyroxene, and euhedral opaques (Iron oxides) and some volcanic glasses. Some of alteration of plagioclase into Calcite and pyroxene into chlorite is observed. glomeroporphyritic texture and some of them shows zoning.
Kote-2	580357E 775907N	Rhyolite	Considering the volume proportionin the groundmass and phynocrysts the rock contains (75 vol. %) euhedral sanadine, (15 vol. %)euhedral to subhedral quartz, (10 vol. %) volcanic glass and (<1%) tiny granules of hornblende. No secondary and opaque minerals exist. The groundmass contains volcanic glass and fine-grained sanadine, quartz and hornblende. The rock shows flow/trachytic texture that appears on the parallel alignments of sanadine minerals in preferred direction.
Din-03b	574659E 770688N	Trachyte	The phenocrysts and groundmass occupy equal proportions (50 vol. %) each. The phenocrysts contain (35 vol. %) euhedral to subhedral sanadine, (15 vol. %) subhedral to anhedral quartz and (1 vol. %) subhedral pyroxene. The groundmass is composed of very fine-grained sanadine, lath-plagioclase, pyroxene, quartz, and volcanic glass and opaque (iron oxides). No secondary minerals observed. The rock texture is flow/trachytic texture defined by sub-parallel alignments of sanadine and some plagioclases.
Kawa-3	576208E 796628N	Porphyritic Basalt	The rock shows porphyritic texture. The phenocrysts and groundmass occupy equal proportions (50 vol. %) each. The phenocrysts contain (35 vol. %) subhedral to anhedral plagioclase, (13 vol. %) subhedral to anhedral pyroxene and (2 vol. %) subhedral olivine. The groundmass is composed of lath-shaped plagioclase, very fine-grained pyroxene, olivine and opaque. Some of the plagioclases show zoning. Little alteration products of calcite and chlorite are observed. The rock texture is porphyritic.

San-2	599990E 760834N	Porphyritic Olivine Basalt	The rock shows porphyritic texture. The phenocrysts cover only (20 vol. %) and groundmass occupy (80 vol. %). The phenocrysts contain (10 vol. %) subhedral to euhedral Plagioclase, (8 vol. %) subhedral to anhedral Pyroxene and (2 vol. %) euhedral Olivine. The (80 vol. %) groundmass is composed of lath-shaped plagioclase, pyroxene, olivine and Subhedral to euhedral opaque. some plagioclase contains perfect rectangular zoning. Very few calcite crystals formed at the expense of plagioclase is observed.
Kawa-1	577140E 795361N	Porphyritic Basalt	The rock shows porphyritic texture. The phenocrysts cover (45 vol. %) and groundmass occupy (65 vol. %). The phenocrysts contain only subhedral to euhedral plagioclases. The groundmass is composed of very fine-grained opaque, lath-plagioclase, pyroxene and calcite. Most of the plagioclases in the phenocrysts and groundmass altered into calcite. The plagioclase shows glomeroporphyritic texture. There are well-developed veins filled with calcite across the thin section, on the grain of plagioclase and as individual crystals. Calcite occur on the grin of plagioclase and as individual crystals. This may indicate weathering intensity is extensive. The oxidized pyroxenes are rimed with iron oxides.
Kawa-4	577585E 794378N	Porphyritic Basalt	The rock shows porphyritic texture. The phenocrysts and groundmass cover equal proportion (50 vol. %)each. The phenocrysts contain (30 vol. %) subhedral to anhedral plagioclase and (20 vol. %) subhedral to anhedral pyroxene. The groundmass is composed of very fine-grained plagioclase, pyroxene, biotite and opaque. The secondary minerals are calcite and chlorite.
Kote-1	584486E 779924N	Rhyolite	The phenocrysts cover (35 vol. %) and groundmass occupy (65 vol. %). The phenocrysts contains (20 vol. %) euhedral sanadine and (15 vol. %) subhedral to euhedral quartz. The groundmass is composed of mainly fine-grained lath-sanadine and very fine-grained quartz, opaque, volcanic glass, hornblende and pyroxene.

Din-07	577308E 772666N	Trachyte	No clear separation between the phenocrysts and the groundmass, euhedral sanadine covers (80 vol. %), subhedral to euhedral quartz (10 vol. %), subhedral to euhedral opaque (3 vol. %), volcanic glass (5 vol. %) and subhedral to euhedral hornblende (2 vol. %). Very few minor crystals of sanadine grow over very fine-grained groundmass that is dominantly covered by lath-sanadine, subhedral to Euhedral quartz, opaque, hornblende and volcanic glass. The texture of the rock is trachytic texture defined by parallel to sub parallel alignments of lath-sanadine. No secondary Minerals.
Bat-01	590419E 754452N	Rhyolite	The volume percent proportion of the phenocrysts and the groundmass. Euhedral sanadine (65 vol. %), euhedral to subhedral quartz (25 vol. %), euhedral to subhedral hornblende (5 vol. %), volcanic glass (5 vol. %), subhedral to anhedral opaque (2 vol. %). No secondary minerals (quite fresh). It shows flow texture defined by parallel to sub parallel alignments of sanadine.

ANNEX 1: Drainage density

POLY_ID	EASTING	NORTHING	D_DEN
1	556051	800686	0.829
2	556051	798686	0.511
3	556051	796686	9.189
4	556051	794686	0.976
5	556051	792686	0.160
6	556051	790686	0.426
7	556051	788686	1.195
8	556051	786686	1.090
9	556051	784686	0.919
10	556051	782686	0.693
11	556051	780686	0.858
12	556051	778686	0.820
13	556051	776686	0.680
14	556051	774686	0.703
15	556051	772686	2.264
16	556051	770686	1.615
17	556051	768686	3.031
18	556051	766686	1.685
19	556051	764686	0.906
20	556051	762686	2.022
21	556051	760686	0.301
22	556051	758686	0.614
23	556051	756686	0.346
24	556051	754686	1.540
25	556051	752686	2.321
26	556051	750686	1.641
27	556051	748686	1.439
28	556051	746686	1.953
29	558051	800686	0.979
30	558051	798686	1.242
31	558051	796686	0.986
32	558051	794686	0.567
33	558051	792686	1.070
34	558051	790686	0.584
35	558051	788686	0.894
36	558051	786686	1.211
37	558051	784686	1.079
38	558051	782686	0.776
39	558051	780686	0.928
40	558051	778686	0.553
41	558051	776686	0.925
42	558051	774686	0.998
43	558051	772686	1.613
44	558051	770686	2.170
45	558051	768686	0.858
46	558051	766686	0.865
47	558051	764686	1.558
48	558051	762686	0.314
49	558051	760686	1.367
50	558051	758686	1.179
51	558051	756686	0.385
52	558051	754686	1.573
53	558051	752686	1.476
54	558051	750686	1.913
55	558051	748686	2.595
56	558051	746686	1.953
57	560051	800686	0.692
58	560051	798686	1.350
59	560051	796686	0.869
60	560051	794686	0.887
61	560051	792686	1.407
62	560051	790686	1.184
63	560051	788686	0.717
64	560051	786686	0.762
65	560051	784686	1.834
66	560051	782686	1.078
67	560051	780686	0.898
68	560051	778686	1.230
69	560051	776686	0.849
70	560051	774686	1.021
71	560051	772686	2.495
72	560051	770686	1.428
73	560051	768686	0.790
74	560051	766686	1.381
75	560051	764686	1.031
76	560051	762686	0.245
77	560051	760686	0.516
78	560051	758686	0.579
79	560051	756686	0.803
80	560051	754686	2.185
81	560051	752686	2.966
82	560051	750686	1.319
83	560051	748686	2.887
84	560051	746686	2.042
85	562051	800686	0.839
86	562051	798686	1.299
87	562051	796686	1.239
88	562051	794686	0.980
89	562051	792686	0.168
90	562051	790686	1.507
91	562051	788686	0.884

92	562051	786686	1.808	140	564051	746686	2.218
93	562051	784686	1.349	141	566051	800686	0.601
94	562051	782686	1.571	142	566051	798686	0.937
95	562051	780686	0.779	143	566051	796686	1.437
96	562051	778686	1.303	144	566051	794686	1.351
97	562051	776686	1.338	145	566051	792686	1.049
98	562051	774686	0.452	146	566051	790686	0.804
99	562051	772686	2.936	147	566051	788686	2.409
100	562051	770686	0.263	148	566051	786686	1.244
101	562051	768686	0.661	149	566051	784686	1.103
102	562051	766686	0.383	150	566051	782686	1.298
103	562051	764686	0.019	151	566051	780686	1.659
104	562051	762686	1.698	152	566051	778686	1.197
105	562051	760686	0.000	153	566051	776686	1.550
106	562051	758686	0.061	154	566051	774686	1.523
107	562051	756686	0.375	155	566051	772686	1.646
108	562051	754686	0.745	156	566051	770686	0.723
109	562051	752686	2.170	157	566051	768686	0.619
110	562051	750686	2.174	158	566051	766686	0.283
111	562051	748686	2.014	159	566051	764686	0.949
112	562051	746686	2.007	160	566051	762686	0.427
113	564051	800686	2.351	161	566051	760686	0.986
114	564051	798686	0.539	162	566051	758686	0.493
115	564051	796686	1.080	163	566051	756686	0.763
116	564051	794686	1.460	164	566051	754686	0.951
117	564051	792686	1.720	165	566051	752686	3.081
118	564051	790686	0.000	166	566051	750686	1.771
119	564051	788686	1.209	167	566051	748686	2.195
120	564051	786686	0.609	168	566051	746686	0.688
121	564051	784686	1.352	169	568051	800686	1.444
122	564051	782686	0.693	170	568051	798686	1.253
123	564051	780686	0.779	171	568051	796686	2.058
124	564051	778686	2.067	172	568051	794686	1.088
125	564051	776686	0.679	173	568051	792686	1.221
126	564051	774686	1.132	174	568051	790686	0.496
127	564051	772686	0.385	175	568051	788686	1.161
128	564051	770686	2.371	176	568051	786686	1.475
129	564051	768686	1.762	177	568051	784686	1.695
130	564051	766686	1.172	178	568051	782686	1.819
131	564051	764686	0.000	179	568051	780686	0.990
132	564051	762686	0.155	180	568051	778686	1.677
133	564051	760686	0.541	181	568051	776686	0.876
134	564051	758686	0.214	182	568051	774686	0.875
135	564051	756686	0.459	183	568051	772686	1.476
136	564051	754686	1.182	184	568051	770686	0.070
137	564051	752686	2.023	185	568051	768686	0.000
138	564051	750686	2.388	186	568051	766686	1.383
139	564051	748686	2.888	187	568051	764686	1.052

188	568051	762686	0.631	236	572051	778686	0.041
189	568051	760686	0.000	237	572051	776686	0.437
190	568051	758686	0.797	238	572051	774686	1.392
191	568051	756686	2.311	239	572051	772686	1.477
192	568051	754686	0.797	240	572051	770686	0.866
193	568051	752686	2.044	241	572051	768686	2.068
194	568051	750686	1.782	242	572051	766686	0.657
195	568051	748686	2.945	243	572051	764686	1.394
196	568051	746686	1.892	244	572051	762686	1.513
197	570051	800686	1.393	245	572051	760686	0.935
198	570051	798686	1.087	246	572051	758686	2.880
199	570051	796686	0.548	247	572051	756686	0.863
200	570051	794686	1.244	248	572051	754686	2.682
201	570051	792686	1.769	249	572051	752686	1.537
202	570051	790686	1.240	250	572051	750686	1.287
203	570051	788686	0.695	251	572051	748686	1.366
204	570051	786686	0.980	252	572051	746686	2.519
205	570051	784686	1.707	253	574051	800686	0.722
206	570051	782686	1.110	254	574051	798686	1.670
207	570051	780686	1.495	255	574051	796686	0.803
208	570051	778686	0.737	256	574051	794686	1.418
209	570051	776686	0.221	257	574051	792686	0.460
210	570051	774686	0.744	258	574051	790686	1.031
211	570051	772686	1.912	259	574051	788686	1.114
212	570051	770686	1.674	260	574051	786686	1.243
213	570051	768686	1.227	261	574051	784686	0.938
214	570051	766686	0.957	262	574051	782686	1.527
215	570051	764686	0.338	263	574051	780686	0.690
216	570051	762686	0.000	264	574051	778686	0.476
217	570051	760686	0.086	265	574051	776686	0.410
218	570051	758686	2.689	266	574051	774686	1.837
219	570051	756686	2.823	267	574051	772686	0.951
220	570051	754686	1.740	268	574051	770686	1.404
221	570051	752686	2.112	269	574051	768686	1.163
222	570051	750686	2.559	270	574051	766686	0.101
223	570051	748686	1.855	271	574051	764686	1.605
224	570051	746686	1.499	272	574051	762686	0.562
225	572051	800686	0.859	273	574051	760686	2.163
226	572051	798686	0.370	274	574051	758686	2.639
227	572051	796686	0.818	275	574051	756686	1.700
228	572051	794686	0.919	276	574051	754686	2.186
229	572051	792686	0.923	277	574051	752686	2.708
230	572051	790686	0.585	278	574051	750686	2.759
231	572051	788686	0.721	279	574051	748686	3.255
232	572051	786686	0.274	280	574051	746686	20.551
233	572051	784686	1.771	281	576051	800686	0.468
234	572051	782686	0.468	282	576051	798686	0.297
235	572051	780686	0.214	283	576051	796686	1.040

284	576051	794686	1.461	332	578051	754686	1.970
285	576051	792686	1.567	333	578051	752686	1.908
286	576051	790686	0.431	334	578051	750686	3.010
287	576051	788686	2.125	335	578051	748686	2.714
288	576051	786686	1.454	336	578051	746686	2.105
289	576051	784686	2.169	337	580051	800686	0.573
290	576051	782686	1.729	338	580051	798686	0.656
291	576051	780686	0.047	339	580051	796686	1.313
292	576051	778686	0.856	340	580051	794686	1.121
293	576051	776686	1.532	341	580051	792686	1.652
294	576051	774686	0.796	342	580051	790686	1.914
295	576051	772686	1.988	343	580051	788686	0.848
296	576051	770686	1.980	344	580051	786686	1.525
297	576051	768686	1.513	345	580051	784686	0.850
298	576051	766686	1.015	346	580051	782686	0.425
299	576051	764686	1.017	347	580051	780686	1.975
300	576051	762686	0.554	348	580051	778686	1.002
301	576051	760686	0.916	349	580051	776686	1.459
302	576051	758686	1.753	350	580051	774686	1.883
303	576051	756686	0.981	351	580051	772686	2.006
304	576051	754686	0.528	352	580051	770686	1.695
305	576051	752686	0.806	353	580051	768686	2.482
306	576051	750686	2.883	354	580051	766686	1.741
307	576051	748686	2.417	355	580051	764686	1.520
308	576051	746686	1.788	356	580051	762686	1.322
309	578051	800686	0.641	357	580051	760686	2.296
310	578051	798686	0.969	358	580051	758686	1.826
311	578051	796686	1.461	359	580051	756686	0.000
312	578051	794686	1.399	360	580051	754686	0.813
313	578051	792686	2.166	361	580051	752686	2.446
314	578051	790686	1.210	362	580051	750686	2.911
315	578051	788686	1.050	363	580051	748686	2.426
316	578051	786686	2.213	364	580051	746686	8.146
317	578051	784686	2.050	365	582051	800686	0.491
318	578051	782686	1.569	366	582051	798686	0.633
319	578051	780686	0.428	367	582051	796686	0.823
320	578051	778686	0.967	368	582051	794686	0.992
321	578051	776686	0.990	369	582051	792686	0.562
322	578051	774686	1.477	370	582051	790686	0.473
323	578051	772686	1.599	371	582051	788686	0.385
324	578051	770686	0.000	372	582051	786686	1.730
325	578051	768686	1.214	373	582051	784686	0.302
326	578051	766686	2.001	374	582051	782686	1.738
327	578051	764686	1.301	375	582051	780686	2.234
328	578051	762686	1.294	376	582051	778686	1.006
329	578051	760686	1.278	377	582051	776686	1.227
330	578051	758686	1.084	378	582051	774686	0.814
331	578051	756686	0.000	379	582051	772686	2.246

380	582051	770686	1.202	428	586051	786686	1.073
381	582051	768686	1.344	429	586051	784686	1.870
382	582051	766686	1.127	430	586051	782686	2.760
383	582051	764686	1.246	431	586051	780686	1.939
384	582051	762686	1.575	432	586051	778686	2.024
385	582051	760686	2.570	433	586051	776686	1.239
386	582051	758686	0.566	434	586051	774686	1.445
387	582051	756686	0.019	435	586051	772686	1.776
388	582051	754686	0.467	436	586051	770686	1.948
389	582051	752686	2.033	437	586051	768686	1.149
390	582051	750686	1.302	438	586051	766686	2.356
391	582051	748686	2.539	439	586051	764686	1.139
392	582051	746686	17.853	440	586051	762686	0.968
393	584051	800686	0.781	441	586051	760686	0.191
394	584051	798686	0.692	442	586051	758686	0.673
395	584051	796686	1.167	443	586051	756686	1.216
396	584051	794686	0.526	444	586051	754686	1.254
397	584051	792686	0.912	445	586051	752686	0.803
398	584051	790686	1.139	446	586051	750686	1.232
399	584051	788686	1.182	447	586051	748686	1.476
400	584051	786686	1.589	448	586051	746686	1.386
401	584051	784686	1.345	449	588051	800686	1.072
402	584051	782686	1.949	450	588051	798686	0.412
403	584051	780686	1.595	451	588051	796686	1.419
404	584051	778686	1.051	452	588051	794686	0.634
405	584051	776686	1.251	453	588051	792686	1.641
406	584051	774686	1.431	454	588051	790686	1.337
407	584051	772686	1.465	455	588051	788686	1.839
408	584051	770686	1.662	456	588051	786686	0.937
409	584051	768686	1.990	457	588051	784686	0.605
410	584051	766686	1.057	458	588051	782686	1.240
411	584051	764686	1.112	459	588051	780686	0.631
412	584051	762686	0.976	460	588051	778686	0.269
413	584051	760686	0.564	461	588051	776686	0.783
414	584051	758686	0.000	462	588051	774686	1.659
415	584051	756686	0.315	463	588051	772686	1.884
416	584051	754686	0.316	464	588051	770686	1.514
417	584051	752686	2.491	465	588051	768686	0.964
418	584051	750686	1.469	466	588051	766686	1.938
419	584051	748686	0.580	467	588051	764686	1.861
420	584051	746686	0.970	468	588051	762686	1.999
421	586051	800686	1.383	469	588051	760686	0.328
422	586051	798686	0.831	470	588051	758686	0.652
423	586051	796686	0.659	471	588051	756686	0.634
424	586051	794686	1.248	472	588051	754686	1.308
425	586051	792686	0.653	473	588051	752686	1.329
426	586051	790686	0.980	474	588051	750686	0.481
427	586051	788686	2.178	475	588051	748686	0.628

476	588051	746686	0.389	524	592051	762686	1.650
477	590051	800686	0.846	525	592051	760686	0.568
478	590051	798686	1.110	526	592051	758686	1.489
479	590051	796686	1.770	527	592051	756686	1.004
480	590051	794686	1.269	528	592051	754686	0.751
481	590051	792686	1.091	529	592051	752686	2.154
482	590051	790686	0.953	530	592051	750686	1.649
483	590051	788686	1.393	531	592051	748686	0.695
484	590051	786686	1.370	532	592051	746686	0.817
485	590051	784686	1.257	533	594051	800686	0.313
486	590051	782686	1.169	534	594051	798686	0.537
487	590051	780686	1.730	535	594051	796686	1.100
488	590051	778686	1.309	536	594051	794686	1.102
489	590051	776686	1.115	537	594051	792686	1.517
490	590051	774686	1.453	538	594051	790686	1.713
491	590051	772686	0.538	539	594051	788686	1.370
492	590051	770686	0.972	540	594051	786686	1.274
493	590051	768686	0.779	541	594051	784686	1.543
494	590051	766686	2.230	542	594051	782686	2.227
495	590051	764686	2.053	543	594051	780686	1.844
496	590051	762686	1.876	544	594051	778686	1.948
497	590051	760686	0.784	545	594051	776686	2.217
498	590051	758686	1.145	546	594051	774686	1.196
499	590051	756686	1.380	547	594051	772686	1.377
500	590051	754686	0.930	548	594051	770686	1.821
501	590051	752686	0.729	549	594051	768686	1.334
502	590051	750686	1.226	550	594051	766686	1.163
503	590051	748686	0.000	551	594051	764686	1.271
504	590051	746686	0.305	552	594051	762686	0.799
505	592051	800686	0.968	553	594051	760686	1.313
506	592051	798686	1.337	554	594051	758686	0.467
507	592051	796686	0.959	555	594051	756686	0.895
508	592051	794686	1.342	556	594051	754686	1.084
509	592051	792686	0.895	557	594051	752686	1.107
510	592051	790686	1.713	558	594051	750686	0.986
511	592051	788686	1.423	559	594051	748686	1.517
512	592051	786686	1.846	560	594051	746686	0.805
513	592051	784686	1.869	561	596051	800686	0.372
514	592051	782686	1.569	562	596051	798686	0.438
515	592051	780686	1.635	563	596051	796686	0.730
516	592051	778686	1.986	564	596051	794686	0.647
517	592051	776686	2.146	565	596051	792686	1.389
518	592051	774686	1.466	566	596051	790686	0.926
519	592051	772686	1.373	567	596051	788686	1.241
520	592051	770686	0.821	568	596051	786686	1.301
521	592051	768686	2.941	569	596051	784686	1.909
522	592051	766686	1.229	570	596051	782686	2.519
523	592051	764686	1.462	571	596051	780686	1.633

572	596051	778686	1.603	620	600051	794686	1.856
573	596051	776686	2.640	621	600051	792686	1.022
574	596051	774686	1.891	622	600051	790686	0.914
575	596051	772686	1.420	623	600051	788686	0.873
576	596051	770686	0.659	624	600051	786686	1.480
577	596051	768686	0.751	625	600051	784686	1.773
578	596051	766686	0.679	626	600051	782686	1.157
579	596051	764686	0.699	627	600051	780686	1.231
580	596051	762686	0.620	628	600051	778686	1.730
581	596051	760686	1.025	629	600051	776686	1.619
582	596051	758686	1.063	630	600051	774686	1.581
583	596051	756686	0.221	631	600051	772686	1.717
584	596051	754686	0.485	632	600051	770686	2.044
585	596051	752686	2.915	633	600051	768686	1.136
586	596051	750686	1.260	634	600051	766686	1.725
587	596051	748686	1.153	635	600051	764686	0.581
588	596051	746686	0.879	636	600051	762686	0.422
589	598051	800686	0.000	637	600051	760686	0.188
590	598051	798686	0.517	638	600051	758686	0.370
591	598051	796686	0.482	639	600051	756686	1.863
592	598051	794686	1.665	640	600051	754686	1.746
593	598051	792686	1.121	641	600051	752686	1.993
594	598051	790686	0.943	642	600051	750686	1.807
595	598051	788686	1.220	643	600051	748686	0.961
596	598051	786686	1.647	644	600051	746686	0.255
597	598051	784686	1.738	645	602051	800686	0.000
598	598051	782686	2.031	646	602051	798686	0.637
599	598051	780686	0.902	647	602051	796686	0.058
600	598051	778686	1.299	648	602051	794686	1.395
601	598051	776686	1.666	649	602051	792686	0.576
602	598051	774686	1.935	650	602051	790686	0.677
603	598051	772686	2.391	651	602051	788686	1.028
604	598051	770686	1.645	652	602051	786686	1.105
605	598051	768686	1.395	653	602051	784686	0.820
606	598051	766686	1.119	654	602051	782686	1.719
607	598051	764686	1.289	655	602051	780686	1.614
608	598051	762686	0.743	656	602051	778686	1.791
609	598051	760686	1.169	657	602051	776686	1.463
610	598051	758686	0.490	658	602051	774686	0.884
611	598051	756686	1.195	659	602051	772686	2.228
612	598051	754686	0.740	660	602051	770686	2.555
613	598051	752686	1.540	661	602051	768686	2.537
614	598051	750686	1.276	662	602051	766686	2.019
615	598051	748686	0.849	663	602051	764686	1.905
616	598051	746686	0.775	664	602051	762686	1.266
617	600051	800686	0.000	665	602051	760686	1.124
618	600051	798686	0.561	666	602051	758686	1.613
619	600051	796686	0.773	667	602051	756686	1.609

668	602051	754686	2.022	716	606051	770686	1.531
669	602051	752686	1.082	717	606051	768686	0.816
670	602051	750686	1.919	718	606051	766686	1.933
671	602051	748686	1.403	719	606051	764686	1.872
672	602051	746686	0.742	720	606051	762686	1.042
673	604051	800686	0.000	721	606051	760686	1.700
674	604051	798686	0.575	722	606051	758686	1.559
675	604051	796686	0.000	723	606051	756686	1.219
676	604051	794686	0.735	724	606051	754686	2.323
677	604051	792686	0.599	725	606051	752686	1.587
678	604051	790686	0.247	726	606051	750686	2.910
679	604051	788686	1.221	727	606051	748686	1.650
680	604051	786686	0.713	728	606051	746686	1.265
681	604051	784686	0.124	729	608051	800686	0.562
682	604051	782686	2.116	730	608051	798686	2.177
683	604051	780686	1.670	731	608051	796686	1.052
684	604051	778686	1.675	732	608051	794686	0.923
685	604051	776686	0.762	733	608051	792686	0.731
686	604051	774686	0.902	734	608051	790686	0.590
687	604051	772686	1.457	735	608051	788686	0.527
688	604051	770686	1.768	736	608051	786686	0.121
689	604051	768686	2.806	737	608051	784686	0.082
690	604051	766686	2.228	738	608051	782686	0.177
691	604051	764686	0.783	739	608051	780686	1.225
692	604051	762686	0.379	740	608051	778686	1.372
693	604051	760686	1.685	741	608051	776686	1.411
694	604051	758686	0.994	742	608051	774686	0.698
695	604051	756686	0.910	743	608051	772686	0.975
696	604051	754686	1.593	744	608051	770686	2.119
697	604051	752686	1.658	745	608051	768686	2.061
698	604051	750686	1.255	746	608051	766686	1.566
699	604051	748686	1.162	747	608051	764686	1.581
700	604051	746686	1.820	748	608051	762686	1.007
701	606051	800686	0.000	749	608051	760686	2.134
702	606051	798686	0.819	750	608051	758686	1.533
703	606051	796686	1.053	751	608051	756686	1.293
704	606051	794686	0.548	752	608051	754686	2.843
705	606051	792686	0.519	753	608051	752686	3.018
706	606051	790686	0.900	754	608051	750686	2.257
707	606051	788686	0.365	755	608051	748686	3.202
708	606051	786686	0.667	756	608051	746686	1.729
709	606051	784686	1.411	757	610051	800686	0.746
710	606051	782686	1.442	758	610051	798686	0.000
711	606051	780686	0.610	759	610051	796686	0.048
712	606051	778686	1.347	760	610051	794686	0.111
713	606051	776686	0.238	761	610051	792686	0.000
714	606051	774686	1.330	762	610051	790686	0.000
715	606051	772686	0.724	763	610051	788686	0.000

764	610051	786686	0.000	812	572051	740686	1.287
765	610051	784686	0.000	813	572051	738686	1.366
766	610051	782686	0.000	814	572051	736686	2.519
767	610051	780686	0.000	815	574051	744686	2.682
768	610051	778686	0.000	816	574051	742686	1.537
769	610051	776686	0.823	817	574051	740686	1.287
770	610051	774686	0.754	818	574051	738686	1.366
771	610051	772686	0.365	819	574051	736686	2.519
772	610051	770686	0.000	820	576051	744686	1.740
773	610051	768686	0.819	821	576051	742686	2.112
774	610051	766686	0.581	822	576051	740686	2.559
775	610051	764686	1.732	823	576051	738686	1.855
776	610051	762686	1.654	824	576051	736686	1.499
777	610051	760686	0.651	825	578051	744686	0.797
778	610051	758686	0.964	826	578051	742686	2.044
779	610051	756686	1.441	827	578051	740686	1.782
780	610051	754686	0.844	828	578051	738686	2.945
781	610051	752686	1.247	829	578051	736686	1.892
782	610051	750686	1.717	830	580051	744686	2.186
783	610051	748686	1.067	831	580051	742686	2.708
784	610051	746686	1.515	832	580051	740686	2.759
785	562051	744686	0.745	833	580051	738686	3.255
786	562051	742686	2.170	834	580051	736686	4.200
787	562051	740686	2.174	835	582051	744686	0.745
788	562051	738686	2.014	836	582051	742686	2.170
789	562051	736686	2.007	837	582051	740686	2.174
790	564051	744686	1.182	838	582051	738686	2.014
791	564051	742686	2.023	839	582051	736686	2.007
792	564051	740686	2.388	840	584051	744686	1.182
793	564051	738686	2.888	841	584051	742686	2.023
794	564051	736686	2.218	842	584051	740686	2.388
795	566051	744686	0.951	843	584051	738686	2.888
796	566051	742686	3.081	844	584051	736686	2.218
797	566051	740686	1.771	845	586051	744686	0.528
798	566051	738686	2.195	846	586051	742686	0.806
799	566051	736686	0.688	847	586051	740686	2.883
800	568051	744686	0.797	848	586051	738686	2.417
801	568051	742686	2.044	849	586051	736686	1.788
802	568051	740686	1.782	850	588051	744686	1.970
803	568051	738686	2.945	851	588051	742686	1.908
804	568051	736686	1.892	852	588051	740686	3.010
805	570051	744686	1.740	853	588051	738686	2.714
806	570051	742686	2.112	854	588051	736686	2.105
807	570051	740686	2.559	855	590051	744686	0.813
808	570051	738686	1.855	856	590051	742686	2.446
809	570051	736686	1.499	857	590051	740686	2.911
810	572051	744686	2.682	858	590051	738686	2.426
811	572051	742686	1.537	859	590051	736686	8.146

860	592051	744686	0.751	883	600051	738686	2.714
861	592051	742686	2.154	884	600051	736686	2.105
862	592051	740686	1.649	885	602051	744686	0.813
863	592051	738686	0.695	886	602051	742686	2.446
864	592051	736686	0.815	887	602051	740686	2.911
865	594051	744686	1.084	888	602051	738686	2.426
866	594051	742686	1.107	889	602051	736686	8.146
867	594051	740686	0.986	890	604051	744686	2.323
868	594051	738686	1.517	891	604051	742686	1.587
869	594051	736686	0.805	892	604051	740686	2.910
870	596051	744686	0.485	893	604051	738686	1.650
871	596051	742686	2.915	894	604051	736686	1.265
872	596051	740686	1.260	895	606051	744686	2.843
873	596051	738686	1.153	896	606051	742686	3.018
874	596051	736686	0.879	897	606051	740686	2.257
875	598051	744686	0.467	898	606051	738686	3.202
876	598051	742686	2.033	899	606051	736686	1.729
877	598051	740686	1.302	900	608051	744686	2.843
878	598051	738686	2.539	901	608051	742686	3.018
879	598051	736686	2.300	902	608051	740686	2.257
880	600051	744686	1.970	903	608051	738686	3.202
881	600051	742686	1.908	904	608051	736686	1.729
882	600051	740686	3.010				

ANNEX 2: Rainfall data

RAINFALL STATIONS	EASTING	NORTHING	PRECIPITATION
Gassera	561844	782558	969.31
Rera	505529	709568	1225.26
Muliyu Burka	643749	718595	1226.59
Robe	610440	782640	835.53
Dinsho	550802	774904	1273.01
Goba	611561	774904	1029.79
Dollo menna	555311	690803	973.73
Sinnana	624809	778250	916.78
Koromi	597003	762039	1061
Tullu Konteh	598782	750313	852
Chorchora	607158	767156	1086

REFERENCES

Abbate, E., Sagri, M., 1969. Dati e considerazioni sul margine orientale dell'altppiano ethiopico nelle province del Tigrai e del Wollo. Boll. Soc. Geol. Ital. 88, 489-497.

Anonymous, 2000, Ethiopian Groundwater Resources Assessment Program (EGRAP), Addis Ababa, p. 1-2,

Baker, J., Snee, L. and Menzies, M. 1996. A brief Oligocene period of flood volcanism in Yemen: implications for the duration and rate of continental flood volcanism at the Afro-Arabian triple junction. Earth and planetary sciences letters, 138, 39-55.

Berhe, S.M., Desta, B., Nicoletti, M. and Tefera, M. (1987). geology, geochronology and geodynamic implications of the Cenozoic magmatic province in W and SE Ethiopia. Jour. Geolo. Soc. Lond., 144, pp. 213-226.

Beyene, S. 1986: A study of some ecological aspects of the Giant Molerat Tachyoryctes macrocephalus in Bale Mountains, Ethiopia. A thesis presented to school of graduate students, Addis Ababa. 90pp, unpubl.

Bonham-Carter, G. F., 1994, Geographic Information System for Geoscientists: modeling with GIS, Pergamon, p. 398.

Carlson, R.W. 1991. Physical and chemical evidence on the cause and source characterstics of flood basalt volcanism. Australian Journal of earth sciences, 38, 525-544.

Chaudhary, B.S.; Kumar, M.; Roy, A.K. and Ruhal D.S. 1996. Application of Remote sensing and Geographic Information Systems in Groundwater investigations in Sohna block, Gurgaon District, Haryana (India). In; International Archives of Photogrametry and Remote sensing Vienna, vol. XXXI, Part B6, pp.18-23.

Chorowicz, J., Collet, B., Bonavia, F.F., Mohr, P., Paarrot, J-F. and Korme, T. 1998, The Tana basin, Ethiopia: Intra-plateau uplift, rifting and subsidence. Tectonphysics, no. 295, p. 351-367.

Crippen, R.E., 1989, Development of remote sensing techniques for the investigation of neotectonic activity, eastern Transverse Ranges and vicinity, southern California, Ph.D. thesis, Univ. of Calif, Sanata Barbara, 304p., 1989b.

Crippen, R. E., R. G. Blom, and J. R. Heyada,1988, Directed band ratioing for the retention of perceptually-independent topographic expression in chromaticity-enhanced imagery, International Journal of Remote Sensing, 9, 749-765.

Davidson and Rex, 1980, D. C., Age of volcanism and rifting in southwestern Ethiopia. Nature, 283, 657-8.

Drury S., 2001 Image interpretation in geology, 3rd edition, Nelson Thornes Ltd, United Kingdom, Blackwell Science Inc., USA, pp. 290

Eberz, G.W., Williams, F. M. and Williams, M. A. J. 1988. Plio-Pleistocene volcanism and sedimentary facies at Gadeb prehistoric site, Ethiopia. Geol. Rund., 77, pp. 513-527.

EIGS. 1998: Geological Map of Dodola at scale of 1:250000; Geological Survey of Ethiopian.

FAO, 2001, Lecture notes on the major soils of the world. Food and Agricultural Organization of the United Nations. Rome, Italy

Gobena H., 2000. Petrology, Geochemistry and Geochronology of Volcanic rock suits of the Dodola area, southeastern Ethiopia. PhD thesis.

Hahn, G.A., Raynolds, R.G.H., Wood, R.A., 1977. The geology of the Angareb ring dike complex, north-western Ethiopia. Bull. Volcanol. 40, 1-10.

Hofmann, A.W. 1997. Mantle geochemistry: the message from oceanic volcanism. Nature, 385, 219-229.

Hofmann, C., Courtillot, V., Feraud, G., Rochette, P., Yirgu, G., Ketefo, E. and Pik, R. 1997. Timing of Ethiopian flood basalt event and implications for plume birth and global change. Nature, 389, 838-841. International Journal of Remote Sensing, 9, 749-765.

Jackson, J.A. 1997. Glossary of geology. Alexandria, Virginia, American Geological Institute.

Justin-Visentin, E., Zanettin, B., 1974.Dike swarms, volcanism and tectonics of the western Afar margin along the Kombolcha-Eloa traverse (Ethiopia). Bull. Volcanol.38, 187-205.

Kennan, P.S., Mitchell, J.G., Mohr, P., 1990.The Sagatu ridge dyke swarm, Ethiopian rift margin: Revised age and new Sr-isotopic data. J. Afr. Earth Sci.11, 39-42.

Kent, R. 1995. Continental and Oceanic flood basalt provinces: current and future prospectives. In: Srivatava, R.K. and Chandra, R. (EDS. (, Mabmatism in relation to diverse tectonic setting. A.A. Balkema, Rotterdam, pp 17-42.

Khan and Mohrana, 2002; Use of Remote sensing and Geographic Information System in the delineation and characterization of groundwater prospect zones, Journal of Indian Society, Remote Sensing, 30(3); 131-141.

Krishnamrthy, J. Venkataesa Kimar, N, Jayraman, V. and Manivel, M. 1996: An approach to demarcate groundwater potential zones through Remote Sensing and Geographic Information System. International Journal of Remote Sensing, Vol. 17, No. 10, p. 1867-1884.

Legg, C. V., 1994, Remote Sensing and Geographic Information Systems: Geological mapping, mineral exploration and mining: John Willey & Sons and Praxis Publishing LTD, p. 59.

Mege, D. and Korme, 2004, Dyke swarm emplacement in the Ethiopian Large Igneous Province: not only a matter of stress.

Mege, D. and Korme, T, 2003, fissure eruption of flood basalts from statistical analysis of dyke fracture length. Journal of Volcanology and Geothermal research, (in press).

Merla, Abbate, E., Canuti, P., Sagri, M. & Tacconi, P. 1979. Geological map of Ethiopia and Somalia. Explanatory notes, Consiglio Nationale delle Richerche, Italy.

Mohr, P. 1983a. Ethiopian flood basalt province. Nature, 303, 577-584.

Mohr, P., 1963. The Ethiopian Cainozoic lavas, a preliminary study of some trends: Spatial, temporal, and chemical. Bull.Geophys. Obs. Addis Ababa 6,103-144.

Mohr, P., 1967.Review of the geology of the Simien Mountains. Bull. Geophys. Obs. Addis Ababa 10, 79-93.

Mohr, P., 1971. Ethiopian Tertiary Dyke Swarms. Smithson. Astrophys. Obs. Spec. Rep. 339, 53 pp.

Mohr, P., 1980. Geochemical aspects of the Sagatu ridge dike swarm, Ethiopian rift margin. In: Geodynamic Evolution of the Afro-Arabian Rift System. Acad. Nat. Lincei, Atti Convegni Lincei 47, pp. 384-067.

Mohr, P., 1983.The Morton-Black hypothesis for the thinning of continental crust-revised in western Afar. Tectonophysics 94, 509-528.

Mohr, P., 1999. The Asmara dike swarm, Eritrean plateau: Physical parameters of an off-rift olivine dolerite injection zone. Acta Vulcanol. 11, 177-181.

Mohr, P., Potter, E.C., 1976. The Sagatu ridge dyke swarm, Ethiopian rift margin. J. Volcanol. Geotherm. Res. 1, 55-71.

Mohr, P., Zanettin, B., 1988. The Ethiopian flood basalt province. In: McDougall, J.D. (Ed.), Continental Flood Basalts.Kluwer, Dordrecht, pp. 63-110.

Potter, E.C., 1975. Pleistocene glaciation in Ethiopia: new evidence. Department of Geology, Oregon University, Massachussets, unpublished report.

Prakash, S.R. 1993. Identification of groundwater prospecting zones by using remote sensing and geo-electrical methods in and around Saidnager area, Dakar Block, jalaun district, U.P., Indian Society of Remote Rensing 21(4):217-227.

Ravindran, K.V. and Jeyram A., 1997. Groundwater prospects of Shahbad tehsil, Baran district and eastern Rajasthan: A remote sensing approach. Indian society of remote sensing 25 (4): 239-246.

Rokos, D., Mavrantza, R., Vamvoukakis, K., St-Seymour, Kouli M., Karfakis, I. and Denes, G., 2000, Localization of ore alteration zoning for the detection of epithermal gold by integration of remote sensing and geochemical

techniques: Proceedings of the Fourteenth International Conference on Applied Geologic Remote Sensing, Las Vegas Nevada, p. 161-168.

Roy, A.K.; and Ray P.K.C., 1993, groundwater investigation using remote sensing and geographic information techniques- A case study in Manabazar-II, Purulia (W.B.). Proceeding national symposium of north-eastern region, Guwahati, India pp. 180-184.

Sabine and Georg Miech, 1994, Ericaceous Forests and Heathlands in the Bale Mountains of South Ethiopia; Ecology and Man's Impact, p 206.

Sabins, F.F., 1999, Remote Sensing for mineral exploration: Ore Geology Reviews, v. 14, p. 157-183.

Saraf and Chaudhary, P.R, 1998: Integrated Remote sensing and Geographic Information System for groundwater exploration and Identification of artificial recharge sites, International Journal of Remote Sensing, Vol. 19, No. 10, p. 1825-1845.

Slate, J. L., M. E. Berry, et al. 1999. Digital geologic map of the Nevada Test Site and vicinity, Nye, Lincoln, and clark countries, Nevada, and inyo country, California, revision 4. Reston, va, United States, U.s. Geological Survey open-file Report 99-554-A.

Stuart Williams, 2002 Bale Mountains a Guidebook, Ethiopian Wolf Conservation Programme.

Tesfaye, K., 1999. Lithologic & Structural Mapping of the Northeastern Lake Ziway area, Ethiopia Rift, with the help of Landsat - TM data, SINET, V.22, No.2, P.175-190.

WBISPP. (1997)Atlas of Woody Biomass Inventory and Strategic Planning Project, South Nations, Nationalities and Peoples Regional State. Ministry of Agriculture.

Yalden, D.W. 1975: Some observation on the Giant molerat Tachyoryctes macrocephalus of Ethiopia. –Monit. zool. Ital. (N.S.) Suppl. VI: 275-303.

Zhang.C, 2002. Applications of remote sensing in Geological Mapping. Dept. Earth and Atmospheric Sciences, Purdue University, West Lafayette, IN 47907, USA.